Signal Recovery on Graphs: Fundamental Limits of Sampling Strategies

Siheng Chen, *Student Member, IEEE*, Rohan Varma, *Student Member, IEEE*, Aarti Singh, Jelena Kovačević, *Fellow, IEEE*

arXiv:1512.05405v2 [cs.IT] 10 Feb 2016

***Abstract*—This paper builds theoretical foundations for the recovery of a newly proposed class of smooth graph signals, approximately bandlimited graph signals, under three sampling strategies: uniform sampling, experimentally designed sampling and active sampling. We then state minimax lower bounds on the maximum risk for the approximately bandlimited class under three sampling strategies and show that active sampling cannot fundamentally outperform experimentally designed sampling. We then propose a recovery strategy to compare uniform sampling with experimentally designed sampling. As the proposed recovery strategy lends itself well to statistical analysis, we derive the exact mean square error of each sampling strategy. To study convergence rates, we introduce two types of graphs and find that (1) the proposed recovery strategies achieve the optimal rates; and (2) the experimentally designed sampling fundamentally outperforms uniform sampling for type-2 class of graphs. To validate our proposed recovery strategies, we test them on five specific graphs: a ring graph with k nearest neighbors, an Erdős-Rényi graph graph, a random geometric graph, a small-world graph and a power-law graph and find that experimental results match the proposed theory well. This work shows a comprehensive explanation for when and why sampling for semi-supervised learning with graphs works.**

***Index Terms*—signal processing on graphs, signal recovery, experimentally designed sampling, active sampling, semi-supervised learning**

I. Introduction

The massive data being generated from various sources, including online social networks, citation networks, biological networks, and physical infrastructures has inspired an emerging field of research on analyzing data supported on graphs [2], [3]. This research is an interdisciplinary field involving a variety of scientific and engineering studies; for example, selecting the representative training data to improve semi-supervised learning with graphs; detecting clusters in communication or social networks and detecting anomaly in sensor networks.

Signal processing on graphs is a theoretical framework for the analysis of high-dimensional data with complex, nonregular structures [4], [5]. This framework extends classical discrete signal processing to signals with an underlying complex, irregular structure. The framework models that underlying structure by a graph and signals by graph signals, generalizing concepts and tools from classical discrete signal processing to graph signal processing. Recent work involves sampling for graph signals [6], [7], [8], recovery for graph signals [9], [10], represents for graph signals [11], [12], uncertainty principles on graphs [13], [14], graph dictionary construction [15], semi-supervised learning with graphs [16], [17], denoising [18], [19], community detection and clustering on graphs [20], [21], [22], graph-based filter banks [18], [23] and graph-based transforms [24], [25], [26].

In this paper, we consider the classical signal processing task of sampling and recovery [27], [28], one of the most critical topics in signal processing. As the bridge connecting sequences and functions, classical sampling theory shows that a bandlimited function can be perfectly recovered from its sampled sequence if the sampling rate is high enough. During the 60 years since Shannon, many new sampling and recovery frameworks emerged to recover signals with different properties with either regular or irregular sampling. To name a few, finite rate of innovation sampling considers the problem of sampling and recovering signals that have a finite number of degrees of freedom per unit time [29], [30], compressed sensing attempts to sample and recover sparse signals or signals that can be sparsely represented by some coherent and redundant dictionary [31], [32], and subspace sampling considers sampling and recovering signals from a union of subspaces [33], [34].

The interest in sampling and recovery of graph signals has increased in the last few years [35], [36], [37], [8], [38]. In [9], authors proposed an algorithm to recover graph signals that have small variation under uniform sampling, with an upper bound of recovery error. In [6], [7], authors proposed a sampling theory for graph signals and show perfect recovery for bandlimited graph signals under experimentally designed sampling. Extensions include a fast distributed algorithm [39], [40], local weighted measurements [41], local aggregation [42] and percolation from seeding nodes [43].

In this paper, we propose a new class of graph signals, called *approximately bandlimited*. We build a theoretical foundation to understand the recovery of this class under uniform sampling, experimentally designed sampling and active sampling. We propose a recovery strategy to compare uniform sampling and experimentally designed sampling, which is an unbiased estimator for low-frequency components and achieves the optimal rate of convergence under some assumption of the graph structures. Our work follows previous work that studied the theoretical capabilities of passive sampling and active sampling for recovering functions from samples [44], [45]. The

S. Chen and R. Varma are with the Department of Electrical and Computer Engineering, Carnegie Mellon University, Pittsburgh, PA, 15213 USA. Emails: sihengc, rohanv@andrew.cmu.edu. A. Singh is with the Department of Machine Learning, Carnegie Mellon University, Pittsburgh, PA, 15213 USA. Email: aarti@cs.cmu.edu. J. Kovačević is with the Departments of Electrical and Computer Engineering and Biomedical Engineering, Carnegie Mellon University, Pittsburgh, PA. Email: jelenak@cmu.edu.

The authors gratefully acknowledge support from the NSF through awards 1130616, 1421919, the University Transportation Center grant (DTRT12-GUTC11) from the US Department of Transportation, and the CMU Carnegie Institute of Technology Infrastructure Award. Parts of this paper appears in [1].

main difference is that we consider a discrete setting and deal with irregular structures. For a smooth function, active sampling, experimentally designed sampling, and uniform sampling have the same performance from a statistical perspective [46], [44]. However, for the approximately bandlimited graph signals, while active sampling has the same rate of convergence as experimentally designed sampling, experimentally designed sampling fundamentally outperforms uniform sampling when the supported graph is irregular.

To validate the recovery strategies, we test them on five specific graphs: a ring graph with k nearest neighbors, an Erdős-Rényi graph, a random geometric graph, a small-world graph and a power-law graph and show that experimental results match the proposed theory well.

Contributions. The contributions of the paper are as follows: We propose

- a new class of smooth graph signals related to existing classes of smooth graph signals;
- minimax lower bounds on the recovery error under three sampling strategies;
- a recovery strategy that achieves optimal rates of convergence on two specific types of graphs;
- a statistical analysis of graph structures; and
- a comprehensive explanation of when and why experimentally designed sampling works for semi-supervised learning with graphs.

Outline of the paper. Section II briefly reviews graph signal processing; Section III reviews smooth graph signal models and formulates sampling and recovery strategies; Section IV proposes the minimax lower bounds on the recovery errors; Section V proposes a recovery strategy that works for both uniform sampling and experimentally designed sampling; Section VI shows the optimal convergence rates of recovery on two types of graphs. The proposed recovery strategies are evaluated in Section VII on five known graph classes. Section VIII concludes the paper and provides pointers to future directions.

II. Signal Processing on Graphs

In this section, we briefly review signal processing on graphs [5], which lays a foundation for the proposed work. We consider a graph $G = (\mathcal{V}, \mathrm{A})$, where $\mathcal{V} = \{v_0, \ldots, v_{N-1}\}$ is the set of nodes and $\mathrm{A} \in \mathbb{R}^{N\times N}$ is the graph shift, or a weighted adjacency matrix. The edge weight $\mathrm{A}_{n,m}$ between nodes v_n and v_m is a quantitative expression of the underlying relation between the nth and the mth node, such as a similarity, a dependency, or a communication pattern. To guarantee that the shifted signal is properly scaled for comparison with the original one [47], we normalize the graph shift such that $|\lambda_{\max}(\mathrm{A})| = 1$. Once the node order is fixed, the graph signal is written as a vector

$$\mathbf{x} \;=\; \left[x_0, x_1, \ldots, x_{N-1}\right]^T \in \mathbb{R}^N.$$

The Jordan decomposition of A is [47]

$$\mathrm{A} = \mathrm{V}\,\Lambda\,\mathrm{U}, \tag{1}$$

where the generalized eigenvectors of A form the columns of matrix V , $\mathrm{U} = \mathrm{V}^{-1}$ (the norm of each column is normalized to one), and $\Lambda \in \mathbb{R}^{N\times N}$ is the block diagonal matrix of corresponding eigenvalues $\lambda_0, \ldots, \lambda_{N-1}$ of A ($1 = \lambda_0 \geq \lambda_1 \geq \ldots, \geq \lambda_{N-1} \geq -1$). These eigenvalues represent frequencies on the graph [47]. The *graph Fourier transform* of $\mathbf{x} \in \mathbb{R}^N$ is

$$\widehat{\mathbf{x}} = \mathrm{U}\,\mathbf{x}. \tag{2}$$

The *inverse graph Fourier transform* is

$$\mathbf{x} = \mathrm{V}\,\widehat{\mathbf{x}} = \sum_{k=0}^{N-1} \widehat{x}_k \mathbf{v}_k,$$

where $\mathbf{v}_k$ is the kth column of V and $\widehat{x}_k$ is the kth component in $\widehat{\mathbf{x}}$. The vector $\widehat{\mathbf{x}}$ in (2) represents the signal's expansion in the eigenvector basis and describes the frequency components of the graph signal $\mathbf{x}$. The inverse graph Fourier transform reconstructs the graph signal by combining graph frequency components. In general, V is not orthonormal; to restrict its behavior, we assume that

$$\alpha_1 \left\|\mathbf{x}\right\|_2^2 \leq \left\|\mathrm{V}\,\mathbf{x}\right\|_2^2 \leq \alpha_2 \left\|\mathbf{x}\right\|_2^2, \quad \text{for all } \mathbf{x} \in \mathbb{R}^N,$$

where $\alpha_1, \alpha_2 > 0$, that is, V is a Riesz basis with stability constants α_1, α_2 [27]. When A represents an undirected graph, we have $\mathrm{U} = \mathrm{V}^T$ and both U and V are orthonormal. For simplicity, we consider A as an undirected graph in this paper. Note that there are other versions of the graph Fourier transform based different approaches to normalize the adjacency matrix, such as the eigenvector matrix of the graph Laplacian matrix [4]. The proposed methods work for all the versions of the graph Fourier transforms.

III. Problem Formulation

We now review three classes of smooth graph signals and show connections between them. We then describe the sampling and recovery strategies of interest, connecting this work to the previous work on sampling theory on graphs in the process.

A. Graph Signal Model

We focus on smooth graph signals, that is, when the signal coefficient at each node is similar to the signal coefficients of its neighbors. In literature [9], [6], two classes of graph signals have been introduced to measure the smoothness on graphs.

Definition 1. A graph signal $\mathbf{x} \in \mathbb{R}^N$ is *globally smooth* on a graph $\mathrm{A} \in \mathbb{R}^{N\times N}$ with parameter $\eta \geq 0$, when

$$\left\|\mathbf{x} - \mathrm{A}\,\mathbf{x}\right\|_2^2 \;\leq\; \eta \left\|\mathbf{x}\right\|_2^2. \tag{3}$$

Denote this class of graph signals by $\mathrm{GS}_{\mathrm{A}}(\eta)$.

Since we normalized the graph shift such that $|\lambda_{\max}(\mathrm{A})| = 1$, $\left\|\mathbf{x} - \mathrm{A}\,\mathbf{x}\right\|_2^2$ is bounded by $4\left\|\mathbf{x}\right\|_2^2$. When $\eta \geq 4$, all graph signals satisfy (3).

Definition 2. A graph signal $\mathbf{x} \in \mathbb{R}^N$ is *bandlimited* on a graph A with parameter $K \in \{0, 1, \cdots, N-1\}$, when the graph frequency components satisfy

$$\widehat{x}_k \;=\; 0 \quad \text{for all} \quad k \geq K.$$

Denote this class of graph signals by $\mathrm{BL}_{\mathrm{A}}(K)$.

Note that the original definition in [6] just requires $\widehat{\mathbf{x}}$ be K-sparse, which is unnecessarily low-pass. Here we fix the ordering of frequencies and requires the bandlimited graph signals be low-pass. To show the relations to these two classes, we present the following theorem.

Theorem 1. For any $K \in \{0, 1, \cdots, N-1\}$, $\mathrm{BL_A}(K)$ is a subset of $\mathrm{GS_A}(\eta)$, when $\eta \geq (1-\lambda_{K-1})^2$.

Proof. Let $\mathbf{x}$ be a graph signal with bandwidth K, that is,

$$\mathbf{x} = \sum_{k=0}^{K-1} \widehat{x}_k \mathbf{v}_k,$$

Then, we write the difference between a signal coefficient and a weighted average of its neighbors as

$$\begin{aligned}
& \left| x_i - \sum_{j \in \mathcal{N}_i} \mathrm{A}_{i,j}\, x_j \right| \\
= & \left| \left(\sum_{k=0}^{K-1} \widehat{x}_k \mathbf{v}_k \right)_i - \sum_{j \in \mathcal{N}_i} \mathrm{A}_{i,j} \left(\sum_{k=0}^{K-1} \widehat{x}_k \mathbf{v}_k \right)_j \right| \\
= & \left| \sum_{k=0}^{K-1} \widehat{x}_k \left((\mathbf{v}_k)_i - \sum_{j \in \mathcal{N}_i} \mathrm{A}_{i,j} (\mathbf{v}_k)_j \right) \right| \\
= & \left| \sum_{k=0}^{K-1} \widehat{x}_k (1-\lambda_k) (\mathbf{v}_k)_i \right| \\
\leq & (1-\lambda_{K-1}) \left| \sum_{k=0}^{K-1} \widehat{x}_k (\mathbf{v}_k)_i \right| \;=\; (1-\lambda_{K-1}) |x_i|.
\end{aligned}$$

The last equality follows from the fact that $\mathbf{v}_k$ and λ_k are eigenvectors and eigenvalues of A. It is clear that for bandlimited graph signals, the signal coefficient at each node is close to the weighted average of all its neighbors; in other words, bandlimited graph signals are smooth locally, which implies global smoothness,

$$\begin{aligned}
\|\mathbf{x} - \mathrm{A}\,\mathbf{x}\|_2^2 \;&=\; \sum_{i=0}^{N-1} |x_i - \sum_{j \in \mathcal{N}_i} \mathrm{A}_{i,j}\, x_j|^2 \\
\leq \; \sum_{i=0}^{N-1} (1-\lambda_{K-1})^2 |x_i|^2 \;&=\; (1-\lambda_{K-1})^2 \|\mathbf{x}\|_2^2 .
\end{aligned}$$

Since a globally smooth graph signal can have isolated high-frequency components, the bandlimited class is a subset of the globally smooth class. □

While the recovery of globally smooth graph signals has been studied in [9] (leading to graph signal inpainting), the globally smooth criterion is quite loose, making it hard to provide further theoretical insight [48]. Similarly, while the recovery of bandlimited graph signals has been studied in [6] (leading to sampling theory on graphs), the bandlimited requirement is a restrictive requirement, making it hard to use in real-world applications. A third class of graph signals is thus proposed that relaxes the bandlimited requirement, but still promote smoothness [1].

Definition 3. A graph signal $\mathbf{x} \in \mathbb{R}^N$ is *approximately bandlimited* on a graph A with parameters $\beta \geq 1$ and $\mu \geq 0$, when there exists a $K \in \{0, 1, \cdots, N-1\}$ such that its graph Fourier transform $\widehat{\mathbf{x}}$ satisfies

$$\sum_{k=K}^{N-1} (1 + k^{2\beta}) \widehat{x}_k^2 \leq \mu \|\mathbf{x}\|_2^2 . \tag{4}$$

Denote this class of graph signals by $\mathrm{ABL_A}(K, \beta, \mu)$.

The approximately bandlimited class allows for a tail after the first K frequency components. The parameter μ controls the shape of the tail; smaller μ means less energy in the tail (high-frequency components). When μ is smaller, we allow fewer energy from the high frequency components. The parameter β controls the speed of energy decay; larger β means higher penalty on the energy from high-frequency components. The class of $\mathrm{ABL_A}(K)$ is similar to the ellipsoid constraints in previous literature [49], where all the frequency components are considered in the constraints; in other words, $\mathrm{ABL_A}(K)$ provides more flexibility for the low-frequency components.

The following theorem shows the relationship between $\mathrm{ABL_A}(K, \beta, \mu)$ and $\mathrm{GS_A}(\eta)$.

Theorem 2. $\mathrm{ABL_A}(K, \beta, \mu)$ is a subset of $\mathrm{GS_A}(\eta)$, when

$$\eta \geq \left(1 - \lambda_{K-1} + \sqrt{\frac{4\mu}{(1+K^{2\beta})}} \right)^2 ;$$

$\mathrm{GS_A}(\eta)$ is a subset of $\mathrm{ABL_A}(K, \beta, \mu)$, when

$$\mu \geq \frac{1 + (N-1)^{2\beta}}{1 - \lambda_K} \eta.$$

From Theorem 2, we see that depending on the parameters, $\mathrm{GS_A}(\eta)$ can be a subset of $\mathrm{ABL_A}(K, \beta, \mu)$ or vice versa.

Proof. To show the first statement, let $\mathbf{x} \in \mathrm{ABL_A}(K, \beta, \mu)$, we have

$$\begin{aligned}
& \|\mathbf{x} - \mathrm{A}\,\mathbf{x}\|_2 \\
= & \left\| \sum_{k=0}^{N-1} \widehat{x}_k \mathbf{v}_k - \mathrm{A} \sum_{k=0}^{N-1} \widehat{x}_k \mathbf{v}_k \right\|_2 \\
\overset{(a)}{\leq} & \left\| \sum_{k=0}^{K-1} \widehat{x}_k \mathbf{v}_k - \mathrm{A} \sum_{k=0}^{K-1} \widehat{x}_k \mathbf{v}_k \right\|_2 \\
& + \left\| \sum_{k=K}^{N-1} \widehat{x}_k \mathbf{v}_k - \mathrm{A} \sum_{k=K}^{N-1} \widehat{x}_k \mathbf{v}_k \right\|_2 \\
\overset{(b)}{\leq} & (1-\lambda_{K-1}) \|\mathbf{x}\|_2 + \sqrt{\alpha_2^2 \sum_{k=K}^{N-1} (1-\lambda_k)^2 \widehat{x}_k^2} \\
= & (1-\lambda_{K-1}) \|\mathbf{x}\|_2 + \sqrt{\sum_{k=K}^{N-1} \frac{(1-\lambda_k)^2}{(1+k^{2\beta})} (1+k^{2\beta}) \widehat{x}_k^2} \\
\overset{(c)}{\leq} & (1-\lambda_{K-1}) \|\mathbf{x}\|_2 + \sqrt{\max_{k \in \{K, \cdots, N-1\}} \frac{(1-\lambda_k)^2}{(1+k^{2\beta})} \mu \|\mathbf{x}\|_2^2} \\
\leq & \left(1 - \lambda_{K-1} + \sqrt{\frac{4\mu}{(1+K^{2\beta})}} \right) \|\mathbf{x}\|_2 ,
\end{aligned}$$

where (a) follows from the triangle inequality, (b) from Theorem 1, and (c) from the property of $\mathrm{ABL_A}(K, \beta, \mu)$. To show

the second statement, let $\mathbf{x} \in \mathrm{GS}_{\mathrm{A}}(\eta)$, we have

$$\begin{aligned} & \sum_{k=K}^{N-1}(1+k^{2\beta})\widehat{x}_k^2 \\ = & \sum_{k=K}^{N-1}\frac{1+k^{2\beta}}{(1-\lambda_k)^2}(1-\lambda_k)^2\widehat{x}_k^2 \\ \leq & \max_{k\in\{K,\cdots,N-1\}}\frac{1+k^{2\beta}}{(1-\lambda_k)^2}\sum_{k=K}^{N-1}(1-\lambda_k)^2\widehat{x}_k^2 \\ \leq & \frac{1+(N-1)^{2\beta}}{(1-\lambda_K)^2}\eta\left\|\mathbf{x}\right\|_2^2, \end{aligned}$$

where the last inequality follows from Theorem 1. □

From Theorem 2, we see that $\mathrm{ABL}_{\mathrm{A}}(K,\beta,\mu)$ is not only more general than $\mathrm{BL}_{\mathrm{A}}(K)$, but describes $\mathrm{GS}_{\mathrm{A}}(\eta)$ in a more controlled fashion. In this paper, we focus on $\mathrm{ABL}_{\mathrm{A}}(K,\beta,\mu)$, and study the recovery performance of this class under three sampling strategies.

B. Sampling & Recovery Strategies

We consider the procedure of sampling and recovery as follows: we sample m coefficients from a graph signal $\mathbf{x} \in \mathbb{R}^N$ with noise to produce a noisy sampled signal $\mathbf{y} \in \mathbb{R}^m$, that is,

$$\mathbf{y} \;=\; \Psi\mathbf{x}+\epsilon \;\equiv\; \mathbf{x}_{\mathcal{M}}+\epsilon, \tag{5}$$

where $\epsilon \sim \mathcal{N}(0,\sigma^2\,\mathrm{I}_{m\times m})$, and $\mathcal{M}=(\mathcal{M}_1,\cdot,\mathcal{M}_m)$ denotes the sequence of sampled indices, or called *sampling set*, and $\mathcal{M}_i \in \{0,1,\cdots,N-1\}$ and $|\mathcal{M}|=m$, and the sampling operator Ψ is a linear mapping from $\mathbb{R}^N$ to $\mathbb{R}^m$, defined as

$$\Psi_{i,j}=\begin{cases} 1, & j=\mathcal{M}_i; \\ 0, & \text{otherwise.}\end{cases} \tag{6}$$

We then interpolate $\mathbf{y}$ to get $\mathbf{x}^* \in \mathbb{R}^N$, which recovers $\mathbf{x}$ either exactly or approximately.

We consider three different sampling strategies:

- *uniform sampling* means that sample indices are chosen from from $\{0,1,\cdots,N-1\}$ independently and randomly;
- *experimentally designed sampling* means that sample indices can be chosen beforehand; and
- *active sampling* means that sample indices can be chosen as a function of the sample points and the samples collected up to that instance, that is, $\mathcal{M}_i$ depends only on $\{\mathcal{M}_j,y_j\}_{j<i}$.

It is clear that uniform sampling is a subset of experimentally designed sampling, which is again a subset of active sampling.

The goal in this paper is to study the fundamental limitations of these three sampling strategies when recovering approximately bandlimited graph signals.

IV. Fundamental Limits of Sampling Strategies

In this section, we study the fundamental limitations of the three sampling strategies for recovering $\mathrm{ABL}_{\mathrm{A}}(K,\beta,\mu)$ by showing minimax lower bounds.

We start by introducing some notation [44].

Definition 4. For any recovery strategy $(\mathbf{x}^*,\mathcal{M})$, and any vector $\mathbf{x} \in \mathbb{R}^N$, we define the risk of the recovery strategy as

$$R(\mathbf{x}^*,\mathcal{M},\mathbf{x}) \;=\; \mathbb{E}_{\mathbf{x},\mathcal{M}}[d^2(\mathbf{x}^*,\mathbf{x})],$$

where $\mathbb{E}_{\mathbf{x},\mathcal{M}}$ is the expectation with respect to the probability measure of $\{x_i,y_i\}_{i\in\mathcal{M}}$. We define the maximum risk of a recovery strategy as $\sup_{\mathbf{x}\in\mathbb{R}^N} R(\mathbf{x}^*,\mathcal{M},\mathbf{x})$.

The goal of this section is to find tight lower bounds for the maximum risk, over all possible recovery strategies, that is, we present lower bounds of the form

$$\inf_{(\mathbf{x}^*,\mathcal{M})\in\Theta}\sup_{\mathbf{x}\in\mathbb{R}^N}\mathbb{E}_{\mathbf{x},\mathcal{M}}[d^2(\mathbf{x}^*,\mathbf{x})] \geq c\phi_m^2, \text{ for all } m\geq m_0, \tag{7}$$

where m is the number of samples, $m_0 \in \mathbb{N}, c>0$ is a constant, ϕ_m is a positive sequence converging to zero, and Θ is the set of all recovery strategies. The sequence ϕ_m^2 is denoted as a lower rate of convergence.

The upper bounds on the maximum risk are usually obtained through explicit recovery strategies, as will be presented in Section V. We present upper bounds of the form

$$\inf_{(\mathbf{x}^*,\mathcal{M})\in\Theta}\sup_{\mathbf{x}\in\mathbb{R}^N}\mathbb{E}_{\mathbf{x},\mathcal{M}}[d^2(\mathbf{x}^*,\mathbf{x})] \leq C\phi_m^2, \quad \forall\; m\geq m_0, \tag{8}$$

where $C>0$. If (7) and (8) both hold, then ϕ_m is said to be the optimal rate of convergence. When talking about optimal rates of convergence, we bound the sequence by a polynomial and make statements of the form: Given $\gamma_1<\gamma<\gamma_2$, a rate of convergence ϕ_m^2 is equivalent to $m^{-\gamma}$ if and only if $m^{-\gamma_2}<\phi_m^2<m^{-\gamma_1}$ for n large enough.

Note that the general bounds are for arbitrary graphs and thus involve parameters that depend on the graph structure; given the graph structure, we can specify the parameters and show explicit rates of convergence, as will be shown in Section VI.

Let $\mathrm{V}_{(2,K)}$ be the sub-matrix of V, consisting of the Kth to the $(2K-1)$th columns of V. Remember that m is the size of the sampling set.

Theorem 3. Given the class $\mathrm{ABL}_{\mathrm{A}}(K,\beta,\mu)$:
(1) Under uniform sampling,

$$\begin{aligned} & \inf_{(\mathbf{x}^*,\mathcal{M})\in\Theta_{\mathrm{rand}}}\sup_{\mathbf{x}\in\mathrm{ABL}_{\mathrm{A}}(K,\beta,\mu)}\mathbb{E}_{\mathbf{x},\mathcal{M}}\left(\frac{\left\|\mathbf{x}^*-\mathbf{x}\right\|_2^2}{\left\|\mathbf{x}\right\|_2^2}\right) \\ \geq & \max_{K\leq\kappa_0\leq N}\frac{c_1\mu}{\kappa_0^{2\beta}}\left(1-\frac{c\mu\left\|\mathbf{x}\right\|_2^2}{\sigma^2\kappa_0^{2\beta+2}N}\left\|\mathrm{V}_{(2,\kappa_0)}\right\|_F^2 m\right), \end{aligned}$$

where $c_1>0$, $0<c<1$, and Θ_{rand} denotes the set of all recovery strategies based on uniform sampling;
(2) Under experimentally designed sampling,

$$\begin{aligned} & \inf_{(\mathbf{x}^*,\mathcal{M})\in\Theta_{\mathrm{exp}}}\sup_{\mathbf{x}\in\mathrm{ABL}_{\mathrm{A}}(K,\beta,\mu)}\mathbb{E}_{\mathbf{x},\mathcal{M}}\left(\frac{\left\|\mathbf{x}^*-\mathbf{x}\right\|_2^2}{\left\|\mathbf{x}\right\|_2^2}\right) \\ \geq & \max_{K\leq\kappa_0\leq N}\frac{c_1\mu}{\kappa_0^{2\beta}}\left(1-\frac{c\mu\left\|\mathbf{x}\right\|_2^2}{\sigma^2\kappa_0^{2\beta+2}}\left\|\mathrm{V}_{(2,\kappa_0)}\right\|_{\infty,2}^2 m\right), \end{aligned}$$

where $c_1>0$, $0<c<1$, and Θ_{exp} denotes the set of all recovery strategies based on experimentally designed sampling;

(3) Under active sampling,

$$\inf_{(\mathbf{x}^*,\mathcal{M})\in\Theta_{\text{active}}} \sup_{\mathbf{x}\in \text{ABL}_\text{A}(K,\beta,\mu)} \mathbb{E}_{\mathbf{x},\mathcal{M}} \left(\frac{\|\mathbf{x}^* - \mathbf{x}\|_2^2}{\|\mathbf{x}\|_2^2} \right)$$
$$\geq \max_{K\leq\kappa_0\leq N} \frac{c_1\mu}{\kappa_0^{2\beta}} \left(1 - \frac{c\mu\,\|\mathbf{x}\|_2^2}{\sigma^2\kappa_0^{2\beta+2}} \left\|\mathrm{V}_{(2,\kappa_0)}\right\|_{\infty,2}^2 m \right),$$

where $c_1 > 0$, $0 < c < 1$, and Θ_{active} denotes the set of all recovery strategies based on active sampling.

See Appendix A in the supporting document for the proof of these results. From Theorem 3, we see that experimentally designed sampling has the same minimax lower bound as active sampling, which means that collecting the feedback before taking samples does not fundamentally improve the recovery performance. We also see that the three minimax lower bounds depend on the properties of $\mathrm{V}_{(2,\kappa_0)}$, which depends on the graph structure. When each row of $\mathrm{V}_{(2,\kappa_0)}$ has roughly similar energy, $\left\|\mathrm{V}_{(2,\kappa_0)}\right\|_F^2$ and $N\left\|\mathrm{V}_{(2,\kappa_0)}\right\|_{\infty,2}^2$ are similar; when the energy is concentrated in a few rows, $N\left\|\mathrm{V}_{(2,\kappa_0)}\right\|_{\infty,2}^2$ is much larger than $\left\|\mathrm{V}_{(2,\kappa_0)}\right\|_F^2$; in other words, the minimax lower bound of experimentally designed sampling is tighter than that of uniform sampling. This happens in many real-world graphs that have complex, irregular structure. The minimax lower bounds thus show the potential advantage of experimentally designed sampling and active sampling over uniform sampling. We will elaborate on this in Sections VI and VII.

V. Recovery Strategy

In the previous section, we presented the minimax lower bounds for each of the three sampling strategies and showed that active sampling cannot fundamentally perform better than experimentally designed sampling. We now propose a recovery strategy for both uniform sampling and experimentally designed sampling and evaluate its statistical properties.

A. Algorithm

To analyze uniform sampling and experimentally designed sampling in a similar manner, we consider *sampling score-based sampling* that unifies both sampling strategies. Sampling score-based sampling means that the sample indices are chosen from an importance sampling distribution that is proportional to some sampling score. Let $\{\pi_i\}_{i=1}^n$ be a set of sampling scores, where π_i denotes the probability to choose the ith sample in each random trial. When the sampling score for each node is the same, it is uniform sampling; when the sampling score for each node is designed based on the graph structure, it is experimentally designed sampling.

For $\text{ABL}_\text{A}(K)$, most of the energy is concentrated in the first K frequency components and the graph signal can be approximately recovered by using those. We consider the following recovery strategy to estimate those frequency components by projecting samples onto a bandlimited space.

Algorithm 1. We sample a graph signal m times. Each time, we independently choose a node $\mathcal{M}_j = i$ with probability π_i, and take a measurement $y_{\mathcal{M}_j}$. Let $\Psi \in \mathbb{R}^{m\times N}$ be the sampling operator and $\mathrm{D} \in \mathbb{R}^{N\times N}$ be a diagonal rescaling matrix with $\mathrm{D}_{i,i} = 1/\sqrt{m\pi_i}$. We recover the original graph signal by solving the following optimization problem:

$$\begin{aligned}\mathbf{x}^*_{\text{SP}} &= \mathrm{V}_{(K)} \arg\min_{\widehat{\mathbf{x}}_{(K)}} \left\|\Psi^T\Psi\,\mathrm{D}^2\,\Psi^T\Psi\mathbf{y} - \mathrm{V}_{(K)}\,\widehat{\mathbf{x}}_{(K)}\right\|_2^2 \\ &= \mathrm{V}_{(K)}\,\mathrm{U}_{(K)}\,\Psi^T\Psi\,\mathrm{D}^2\,\Psi^T\Psi\mathbf{y}, \end{aligned} \tag{9}$$

where $\mathbf{y}$ is a vector representation of the samples (5).

We call Algorithm 1 *sampled projection* (SampleProj) because we reweight and project the samples onto the bandlimited space. $\Psi^T\Psi$ chooses samples from $\mathbf{y}$ and the corresponding columns from $\mathrm{U}_{(K)}$. The rescaling matrix D^2 equalizes samples from different sampling scores. The term $\mathrm{U}_{(K)}\,\Psi^T\Psi\,\mathrm{D}^2\,\Psi^T\Psi\mathbf{y}$ is an unbiased estimator for the first K frequency components, which will be shown later. Thus, in expectation, the recovered graph signal $\mathbf{x}^*_{\text{SP}}$ is a linear approximation of any graph signal $\mathbf{x}$. When $\mathbf{x}$ is bandlimited, $\mathbf{x}^*_{\text{SP}}$ perfectly recovers $\mathbf{x}$; when $\mathbf{x}$ is approximately bandlimited, $\mathbf{x}^*_{\text{SP}}$ has a bias due to the high-frequency components.

It is also intuitive to consider the following recovery strategy [50]

$$\begin{aligned}\mathbf{x}^*_{\text{LS}} &= \mathrm{V}_{(K)} \arg\min_{\widehat{\mathbf{x}}_{(K)}} \left\|\mathrm{D}\,\Psi^T\Psi\mathbf{y} - \mathrm{D}\,\Psi^T\Psi\,\mathrm{V}_{(K)}\,\widehat{\mathbf{x}}_{(K)}\right\|_2^2 \\ &= \mathrm{V}_{(K)} \left(\mathrm{D}^2\,\Psi^T\Psi\,\mathrm{V}_{(K)}\right)^\dagger \mathrm{D}\,\Psi^T\Psi\mathbf{y},\end{aligned}$$

where we fit the sampled elements of the recovered graph signal to the samples by solving the least squares problem. The corresponding expected recovered graph signal is

$$\mathbb{E}\mathbf{x}^*_{\text{LS}} = \mathrm{V}_{(K)}\,\widehat{\mathbf{x}}_{(K)} + \mathrm{V}_{(K)}\,\mathrm{P}\,\mathrm{V}_{(-K)}\,\widehat{\mathbf{x}}_{(-K)},$$

where $\mathrm{P} = \left(\mathrm{D}^2\,\Psi^T\Psi\,\mathrm{V}_{(K)}\right)^\dagger \mathrm{D}\,\Psi^T\Psi = \left(\mathrm{U}_{(K)}\,\Psi^T\Psi\,\mathrm{D}^2\,\Psi^T\Psi\,\mathrm{V}_{(K)}\right)^{-1}\mathrm{U}_{(K)}\,\Psi^T\Psi\,\mathrm{D}^2\,\Psi^T\Psi$, $\mathrm{V}_{(-K)}$ is V except for the first K columns, and $\widehat{\mathbf{x}}_{(-K)}$ is $\mathbf{x}$ except for the first K components. When $\mathbf{x}$ is bandlimited, $\mathbf{x}^*_{\text{LS}}$ perfectly recovers $\mathbf{x}$; when $\mathbf{x}$ is approximately bandlimited, however, $\mathbf{x}^*_{\text{LS}}$ is a mixture of low-frequency and high-frequency components and it is hard to show its statistical properties. Compared with computing $\mathbf{x}^*_{\text{SP}}$, it is moreover computationally inefficient to compute $\mathbf{x}^*_{\text{LS}}$ because of the inverse term.

The definitions of the bandlimited class and the approximately bandlimited class and the proposed sampling strategies are all based on the graph Fourier transform instead of on graph shift; thus, all the proposed methods work for other versions of the graph Fourier transform as well.

B. Statistical Analysis

We study the statistical properties of Algorithm 1 by providing the bias, covariance, mean square error (MSE), and an optimal sampling distribution.

Lemma 1 shows that the sampled projection estimator is an unbiased estimator of the first K frequency components for any sampling scores.

Lemma 1. The sampled projection estimator with bandwidth K and arbitrary sampling scores is an unbiased estimator of the first K frequency components, that is,

$$\mathbb{E}\mathbf{x}^* \;=\; \mathrm{V}_{(K)}\,\mathrm{U}_{(K)}\,\mathbf{x}, \text{ for all } \mathbf{x},$$

where $\mathbf{x}^*$ is the solution of Algorithm 1.

Lemma 2 gives the exact covariance of the sampled projection estimator.

Lemma 2. The covariance of sampled projection estimator $\mathbf{x}^*$ has the following property:

$$\begin{aligned}\mathrm{Tr}(\mathrm{Covar}\left[\mathbf{x}^*\right]) &= \mathbb{E}\left\|\mathbf{x}^* - \mathbb{E}\left[\mathbf{x}^*\right]\right\|_2^2 \\ &= \mathrm{Tr}\left(\mathrm{U}_{(K)}\,\mathrm{W}_C\,\mathrm{V}_{(K)}\right) - \frac{1}{m}\left\|\widehat{\mathbf{x}}_{(K)}\right\|_2^2,\end{aligned}$$

where W_C is a diagonal matrix with $(\mathrm{W}_C)_{i,i} = (x_i^2 + \sigma^2)/(m\pi_i)$.

Theorem 4 shows the exact MSE of sampled projection estimator and an upper bound.

Theorem 4. For $\mathbf{x} \in \mathrm{ABL}_{\mathrm{A}}(K, \beta, \mu)$, let $\mathbf{x}^*$ be the sampled projection estimator with bandwidth $\kappa \geq K$. Then,

$$\begin{aligned}&\mathbb{E}\left\|\mathbf{x}^* - \mathbf{x}\right\|_2^2 \\ =\;& \left\|\mathrm{V}_{(-\kappa)}\,\widehat{x}_{(-\kappa)}\right\|_2^2 + \mathrm{Tr}\left(\mathrm{U}_{(\kappa)}\,\mathrm{W}_C\,\mathrm{V}_{(\kappa)}\right) - \frac{1}{m}\left\|\widehat{\mathbf{x}}_{(\kappa)}\right\|_2^2 \\ \leq\;& \frac{\mu}{1+\kappa^{2\beta}}\left\|\mathbf{x}\right\|_2^2 + \mathrm{Tr}\left(\mathrm{U}_{(\kappa)}\,\mathrm{W}_C\,\mathrm{V}_{(\kappa)}\right).\end{aligned}$$

We merge the proofs of Lemmas 1 , 2 and Theorem 4 in Appendix B in the supporting document. The main idea follows from the bias-variance tradeoff. The bias term $\mu/(1+\kappa^{2\beta})\left\|\mathbf{x}\right\|_2^2$ comes from the high-frequency components and $\mathrm{Tr}\left(\mathrm{U}_{(\kappa)}\,\mathrm{W}_C\,\mathrm{V}_{(\kappa)}\right)$ comes from the covariance.

We next study the MSEs of sampled projection estimator based on both uniform sampling and experimentally designed sampling.

Corollary 1. The upper bound of MSE of uniform sampling is

$$\mathbb{E}\left\|\mathbf{x}^* - \mathbf{x}\right\|_2^2 \;\leq\; \frac{\mu}{1+\kappa^{2\beta}}\left\|\mathbf{x}\right\|_2^2 + \frac{N}{m}\sum_{k=1}^{\kappa}\sum_{i=1}^{N}\mathrm{U}_{k,i}^2\left(x_i^2+\sigma^2\right).$$

The upper bound just specifies that the sampling score be $\pi_i = 1/N$ for all i. For experimentally designed sampling, we are allowed to study the graph structure and design sampled indices. In the following corollary, we show a set of optimal sampling scores of the sampled projection estimator by minimizing the upper bound of MSE.

Corollary 2. The optimal sampling score of the sampled projection estimator with bandwidth $\kappa \geq K$ is

$$\pi_i \;\propto\; \sqrt{\left(\sum_{k=1}^{\kappa}\mathrm{U}_{k,i}^2\right)(x_i^2+\sigma^2)}.$$

The corresponding upper bound of MSE is

$$\begin{aligned}&\mathbb{E}\left\|\mathbf{x}^* - \mathbb{E}\mathbf{x}^*\right\|_2^2 \\ \leq\;& \frac{\mu}{1+\kappa^{2\beta}}\left\|\mathbf{x}\right\|_2^2 + \frac{1}{m}\left(\sum_{i=1}^{N}\sqrt{\sum_{k=1}^{\kappa}\mathrm{U}_{k,i}^2\left(x_i^2+\sigma^2\right)}\right)^2.\end{aligned}$$

Proof. To obtain the optimal sampling score for the estimator, we solve the following optimization problem.

$$\begin{aligned}&\min_{\pi_i}\mathrm{Tr}\left(\mathrm{U}_{(\kappa)}\,\mathrm{W}_C\,\mathrm{V}_{(\kappa)}\right), \\ &\text{subject to}: \sum_i \pi_i = 1, \pi_i \geq 0.\end{aligned}$$

The objective function is the upper bound on the MSE of the estimator derived in Theorem 4 and the constraints require $\{\pi_i\}_{i=1}^N$ to be a valid probability distribution. The Lagrangian function is then

$$\begin{aligned}L(\pi_i, \lambda_0, \lambda_i) &= \sum_{i=1}^{N}\left(\frac{x_i^2+\sigma^2}{m\pi_i}\sum_{k=1}^{\kappa}\mathrm{U}_{k,i}^2\right) \\ &\quad +\lambda_0\left(\sum_{i=1}^{N}\pi_i - 1\right) + \sum_{i=1}^{N}\lambda_i\pi_i.\end{aligned}$$

We set the derivative of the Lagrangian function to zero,

$$\frac{dL}{d\pi_i} \;=\; -\frac{x_i^2+\sigma^2}{m\pi_l^2}\sum_{k=1}^{\kappa}\mathrm{U}_{k,i}^2 + \lambda_0 + \lambda_i = 0,$$

and obtain the optimal sampling score

$$\pi_i \;\propto\; \sqrt{\left(\sum_{k=1}^{\kappa}\mathrm{U}_{k,i}^2\right)(x_i^2+\sigma^2)}.$$

Substituting plugin the optimal sampling score π_i to the upper bound of the MSE,

$$\begin{aligned}&\mathbb{E}\left\|\mathbf{x}^* - \mathbb{E}\mathbf{x}^*\right\|_2^2 \;\leq\; \frac{\mu}{1+\kappa^{2\beta}}\left\|\mathbf{x}\right\|_2^2 \\ +\;& \frac{1}{m}\sum_{i=1}^{N}\frac{\sum_{k=1}^{\kappa}\mathrm{U}_{k,i}^2(\sigma^2+x_i^2)}{\sqrt{\sum_{k=1}^{\kappa}\mathrm{U}_{k,i}^2\left(x_i^2+\sigma^2\right)}}\sum_{i=1}^{N}\sqrt{\sum_{k=1}^{\kappa}\mathrm{U}_{k,i}^2\left(x_i^2+\sigma^2\right)} \\ \leq\;& \frac{\mu}{1+\kappa^{2\beta}}\left\|\mathbf{x}\right\|_2^2 + \frac{1}{m}\left(\sum_{i=1}^{N}\sqrt{\sum_{k=1}^{\kappa}\mathrm{U}_{k,i}^2\left(x_i^2+\sigma^2\right)}\right)^2.\end{aligned}$$

□

We see that the optimal sampling score includes a tradeoff between the signal and the noise. In practice, we cannot access $\mathbf{x}$ and thus need to approximate the ratio between each x_i and σ^2. For active sampling, we can collect the feedback to approximate each signal coefficient x_i; for experimentally designed sampling, we approximate beforehand. One way is to use the graph structure to sketch the shape of $\mathbf{x}$. We first use the Cauchy-Schwarz inequality to bound x_i,

$$|x_i| \;=\; |\mathbf{v}_i^T\widehat{\mathbf{x}}| \;\leq\; \left\|\mathbf{v}_i\right\|_2\left\|\widehat{\mathbf{x}}\right\|_2 \;=\; \left\|\mathbf{v}_i\right\|_2\left\|\mathbf{x}\right\|_2,$$

where $\mathbf{v}_i$ is the $i$the row of V. Thus, in the upper bound, we have a tradeoff between the signal and noise: when the signal-to-noise ratio (SNR) $\left\|\mathbf{x}\right\|_2/\sigma^2$ is small, the approximate optimal sampling score is

$$\pi_i \;\propto\; \left\|\mathbf{v}_{i,(K)}\right\|_2 \;=\; \sqrt{\sum_{k=1}^{\kappa}\mathrm{U}_{k,i}^2},$$

which is the square root of the leverage score of $\mathrm{V}_{(K)}$.

When the SNR $\|\mathbf{x}\|_2/\sigma^2$ is large, the approximate optimal sampling score is

$$\pi_i \propto \sqrt{\left(\sum_{k=1}^{\kappa} \mathrm{U}_{k,i}^2\right) \|\mathbf{v}_i\|_2^2}.$$

For approximately bandlimited signals, when β is large and μ is small, the main energy concentrates in the first K frequency components, $\|\mathbf{v}_i\|_2$ is concentrated in $\left\|\mathbf{v}_{i,(K)}\right\|_2$, where $\mathbf{v}_{i,(K)}$ is the first K elements in $\mathbf{v}_i$. To be specific,

$$\begin{aligned} |x_i| &= |\mathbf{v}_i^T \widehat{\mathbf{x}}| = |\mathbf{v}_{i,(K)}^T \widehat{\mathbf{x}}_{(K)} + \mathbf{v}_{i,(-K)}^T \widehat{\mathbf{x}}_{(-K)}| \\ &\leq \left\|\mathbf{v}_{i,(K)}\right\|_2 \left\|\widehat{\mathbf{x}}_{(K)}\right\|_2 + \left\|\mathbf{v}_{i,(-K)}\right\|_2 \left\|\widehat{\mathbf{x}}_{(-K)}\right\|_2 \\ &\leq \left\|\mathbf{v}_{i,(K)}\right\|_2 \left\|\widehat{\mathbf{x}}_{(K)}\right\|_2 + \left\|\mathbf{v}_{i,(-K)}\right\|_2 \sqrt{\frac{\mu}{1+K^{2\beta}}} \|\mathbf{x}\|_2 \\ &\approx \left\|\mathbf{v}_{i,(K)}\right\|_2 \left\|\widehat{\mathbf{x}}_{(K)}\right\|_2. \end{aligned}$$

In this case, when the SNR $\|\mathbf{x}\|_2/\sigma^2$ is large, the approximate optimal sampling score is

$$\pi_i \propto \left\|\mathbf{v}_{i,(K)}\right\|_2^2 = \sum_{k=1}^{\kappa} \mathrm{U}_{k,i}^2,$$

which is the leverage score of $\mathrm{V}_{(K)}$.

C. Relation to Sampling Theory on Graphs

Sampling theory on graphs considers a bandlimited graph signal under the experimentally designed sampling [6]. It shows that for a noiseless bandlimited graph signal, the experimentally designed sampling guarantees perfect recovery, while uniform sampling cannot, which also implies that active sampling cannot perform better than experimentally designed sampling. The recovery strategy is to solve the following optimization problem,

$$\begin{aligned} \mathbf{x}_{\mathrm{ST}}^* &= \arg\min_{\mathbf{x} \in \mathrm{BL}_{\mathrm{A}}(K)} \|\Psi\mathbf{x} - \mathbf{y}\|_2^2 \qquad (10) \\ &= \mathrm{V}_{(K)} (\Psi\, \mathrm{V}_{(K)})^{\dagger} \mathbf{y}, \end{aligned}$$

where Ψ is the sampling operator (6), $\mathbf{y}$ is a vector representation of the samples (5), and $(\cdot)^{\dagger}$ is the pseudo-inverse. When the original graph signal is bandlimited, $\mathbf{x} \in \mathrm{BL}_{\mathrm{A}}(K)$, the solution of (10) is unbiased to estimate the original graph signal $\mathbf{x}$ on expectation and the MSE only comes from the variance introduced by noise, that is,

$$\begin{aligned} & \mathbb{E}\,\|\mathbf{x}_{\mathrm{ST}}^* - \mathbf{x}\|_2^2 \\ = \;& \mathbb{E}\left\|\mathrm{V}_{(K)} (\Psi\, \mathrm{V}_{(K)})^{\dagger} (\Psi\mathbf{x} + \epsilon) - \mathbf{x}\right\|_2^2 \\ = \;& \mathbb{E}\left\|\mathrm{V}_{(K)} (\Psi\, \mathrm{V}_{(K)})^{\dagger} \epsilon\right\|_2^2 = \mathbb{E}\left\|(\Psi\, \mathrm{V}_{(K)})^{\dagger} \epsilon\right\|_2^2. \end{aligned}$$

In [6], the authors propose an optimal sampling operator based on minimizing $\left\|(\Psi\, \mathrm{V}_{(k)})^{\dagger}\right\|_2^2$. The sample set is deterministic and the procedure is computationally efficient when the sample size is small. Compared with sampling score-based sampling, however, the optimal sampling operator is computationally inefficient when the sample size is large. When the original graph signal is not bandlimited, similarly to $\mathbf{x}_{\mathrm{LS}}^*$, the solution of (10) is biased, that is,

$$\begin{aligned} \mathbb{E}\mathbf{x}^* &= \mathrm{V}_{(K)} (\Psi\, \mathrm{V}_{(K)})^{\dagger} \mathbb{E}(\Psi\mathbf{x} + \epsilon) \\ &= \mathrm{V}_{(K)} (\Psi\, \mathrm{V}_{(K)})^{\dagger} \Psi \left(\mathrm{V}_{(K)}\, \widehat{\mathbf{x}}_{(K)} + \mathrm{V}_{(-K)}\, \widehat{\mathbf{x}}_{(-K)}\right) \\ &= \mathrm{V}_{(K)}\, \widehat{\mathbf{x}}_{(K)} + \mathrm{V}_{(K)} (\Psi\, \mathrm{V}_{(K)})^{\dagger}\, \mathrm{V}_{(-K)}\, \widehat{\mathbf{x}}_{(-K)}. \end{aligned}$$

We see that the high-frequency components are reconstructed in a low-frequency space.

VI. Optimal Rates of Convergence

In this section, we introduce two types of graphs and show that the proposed recovery strategies achieve the optimal rates of convergence on both.

A. Type-1 Graphs

Definition 5. A graph $\mathrm{A} \in \mathbb{R}^{N \times N}$ is of *type-1*, when its graph Fourier transform matrix satisfies

$$|\,\mathrm{V}_{i,j}\,| = O(N^{-1/2}), \quad \text{for all } i,j = 0,1,\cdots,N-1.$$

For a type-1 graph, elements in V have roughly similar magnitudes, that is, the energy is evenly spread over V. Some examples are circulant graphs and nearest-neighbor graphs [51].

Based on Theorem 4, we can specify the parameters for a type-1 graph and show the following results.

Corollary 3. Let $\mathrm{A} \in \mathbb{R}^{N \times N}$ be a type-1 graph, for the class $\mathrm{ABL}_{\mathrm{A}}(K, \beta, \mu)$.

- Let $\mathbf{x}^*$ be the sampled projection estimator with the bandwidth $\kappa \geq K$ and uniform sampling; we have
$$\mathbb{E}\left(\frac{\|\mathbf{x}^* - \mathbf{x}\|_2^2}{\|\mathbf{x}\|_2^2}\right) \leq C m^{-\frac{2\beta}{2\beta+1}},$$
where $C > 0$, and the rate is achieved when κ is in the order of $m^{1/(2\beta+1)}$ and upper bounded by N;
- Let $\mathbf{x}^*$ be the sampled projection estimator with the bandwidth $\kappa \geq K$ and the optimal sampling score in Corollary 2; we have
$$\mathbb{E}\left(\frac{\|\mathbf{x}^* - \mathbf{x}\|_2^2}{\|\mathbf{x}\|_2^2}\right) \leq C m^{-\frac{2\beta}{2\beta+1}},$$
where $C > 0$, and the rate is achieved when κ is in the order of $m^{1/(2\beta+1)}$ and upper bounded by N.

When $m \gg N$, we set $\kappa = N$, the bias term is then zero, and both upper bounds are actually Cm^{-1}. We see that uniform sampling and optimal sampling score based sampling have the same convergence rate, that is, experimentally designed sampling does not perform better than uniform sampling for the type-1 graphs.

Based on Theorem 3 and Corollary 3, we conclude the following.

Corollary 4. Let $\mathrm{A} \in \mathbb{R}^{N \times N}$ be a type-1 graph, for the class $\mathrm{ABL}_{\mathrm{A}}(K, \beta, \mu)$.

- Under uniform sampling,

$$cm^{-\frac{2\beta}{2\beta+1}} \leq \inf_{(\mathbf{x}^*,\mathcal{M})\in\Theta_{\text{rand}}} \sup_{\mathbf{x}\in \text{ABL}_\text{A}(K,\beta,\mu)} \mathbb{E}_{\mathbf{x},\mathcal{M}}\left(\|\mathbf{x}^*-\mathbf{x}\|_2^2\right) \leq Cm^{-\frac{2\beta}{2\beta+1}},$$

  where $C > c > 0$, and the rate is achieved when κ is in the order of $m^{1/(2\beta+1)}$ and upper bounded by N;
- Under experimentally designed sampling,

$$cm^{-\frac{2\beta}{2\beta+1}} \leq \inf_{(\mathbf{x}^*,\mathcal{M})\in\Theta_{\text{exp}}} \sup_{\mathbf{x}\in \text{ABL}_\text{A}(K,\beta,\mu)} \mathbb{E}_{\mathbf{x},\mathcal{M}}\left(\|\mathbf{x}^*-\mathbf{x}\|_2^2\right) \leq Cm^{-\frac{2\beta}{2\beta+1}},$$

  where $C > c > 0$, and the rate is achieved when κ is in the order of $m^{1/(2\beta+1)}$ and upper bounded by N.

We merge the proofs of Corollaries 3 and 4 in Appendix C in the supporting document.

We see that in both the random and experimentally designed sampling settings, the lower and upper bounds have the same rate of convergence, which achieves the optimum. In addition, random and experimentally designed sampling have the same optimal rate of convergence and we can thus conclude that experimentally designed sampling does not perform asymptotically better than uniform sampling for the type-1 graphs. The sampled projection estimator attains the optimal rate of convergence.

B. Type-2 Graphs

Definition 6. A graph $\text{A} \in \mathbb{R}^{N\times N}$ is of *type-2*, when its graph Fourier transform matrix satisfies

$$|\mathbf{v}_{i,T}| = O(1), \text{and } |\mathbf{v}_{i,T+1}| \ll O(1), \text{ for all } i = 0, \cdots, N-1,$$

where $\mathbf{v}_{i,T}$ is the Tth largest elements in the ith column of V and $T \ll N$ is some constant.

A type-2 graph requires that each column vector of V is approximately sparse. When we take a few columns from V to form a submatrix, the energy in the submatrix concentrates in a few rows of the submatrix. This is equivalent to the sampling scores being approximately sparse. Simulations show that star graphs, scale-free graphs, small-world graphs approximately fall into this type of graphs.

Based on Theorem 4, we can specify the parameters for a type-2 graph and show the following results.

Corollary 5. Let $\text{A} \in \mathbb{R}^{N\times N}$ be a type-2 graph, for the class $\text{ABL}_\text{A}(K,\beta,\mu)$.

- Let $\mathbf{x}^*$ be the sampled projection estimator with the bandwidth $\kappa \geq K$ and uniform sampling; we have

$$\mathbb{E}\left(\frac{\|\mathbf{x}^*-\mathbf{x}\|_2^2}{\|\mathbf{x}\|_2^2}\right) \leq Cm^{-\frac{2\beta}{2\beta+\gamma}},$$

  where $C > 0$, and the rate is achieved when κ is in the order of $m^{1/(2\beta+\gamma)}$, $\gamma = \log(N)/\log(\kappa) \geq 1$;
- Let $\mathbf{x}^*$ be the sampled projection estimator with the bandwidth $\kappa \geq K$ and optimal sampling score based sampling; we have

$$\mathbb{E}\left(\frac{\|\mathbf{x}^*-\mathbf{x}\|_2^2}{\|\mathbf{x}\|_2^2}\right) \leq Cm^{-\frac{2\beta}{2\beta+1}},$$

  where $C > 0$, the rate is achieved when κ is in the order of $m^{1/(2\beta+1)}$ and upper bounded by N.

Based on Theorem 3 and Corollary 5, we conclude the following.

Corollary 6. Let $\text{A} \in \mathbb{R}^{N\times N}$ be a type-2 graph with parameter K_0, for the class $\text{ABL}_\text{A}(K,\beta,\mu)$.

- Under uniform sampling,

$$cm^{-\frac{2\beta}{2\beta+1}} \leq \inf_{(\mathbf{x}^*,\mathcal{M})\in\Theta_{\text{rand}}} \sup_{\mathbf{x}\in \text{ABL}_\text{A}(K,\beta,\mu)} \mathbb{E}_{\mathbf{x},\mathcal{M}}\left(\frac{\|\mathbf{x}^*-\mathbf{x}\|_2^2}{\|\mathbf{x}\|_2^2}\right) \leq Cm^{-\frac{2\beta}{2\beta+\gamma}},$$

  where $C > c > 0$, and the rate is achieved when κ is in the order of $m^{1/(2\beta+\gamma)}$ and $\gamma = \log(N)/\log(\kappa) \geq 1$;
- Under experimentally designed sampling, there exists a $\gamma > 1$,

$$cm^{-\frac{2\beta}{2\beta+1}} \leq \inf_{(\mathbf{x}^*,\mathcal{M})\in\Theta_{\text{exp}}} \sup_{\mathbf{x}\in \text{ABL}_\text{A}(K,\beta,\mu)} \mathbb{E}_{\mathbf{x},\mathcal{M}}\left(\frac{\|\mathbf{x}^*-\mathbf{x}\|_2^2}{\|\mathbf{x}\|_2^2}\right) \leq Cm^{-\frac{2\beta}{2\beta+1}},$$

  where $C > 0$, the rate is achieved when κ is in the order of $m^{1/(2\beta+1)}$ and upper bounded by N.

We merge the proofs of Corollaries 5 and 6 in Appendix D in the supporting document.

We see that under both the uniform and experimentally designed sampling settings, the lower and upper bounds have the same rate of convergence, which achieves the optimum. However, experimentally designed sampling has a larger optimal rate of convergence, and consequently we can conclude that experimentally designed sampling exhibits asymptotically better performance than uniform sampling for a type-2 graph. The sampled projection estimator attains the optimal rate of convergence.

VII. Experimental Results

In this section, we validate the proposed recovery strategy on five specific graphs: a ring graph, an Erdős-Rényi graph, a random geometric graph, a small-world graph and a power-law graph. Based on the graph structure, we roughly label each as a type-1 or type-2, and then, for each, we compare the empirical performance of the proposed recovery strategy based on uniform and experimentally designed sampling. For experimentally designed sampling, we use both the leverage score of $\text{V}_{(K)}$ (approximately optimal in the noiseless case) and the square root of the leverage score of $\text{V}_{(K)}$ (approximately optimal in the noisy case). In the experiments, the

graph Fourier transform matrix is the eigenvector matrix of the adjacency matrix. We find similar results when the graph Fourier transform matrix is the eigenvector matrix of the graph Laplacian matrix.

A. Simulated Graphs

We now introduce the five graphs, each with $10,000$ nodes, used in our experiments.

Ring graph with k-nearest neighbors. A ring graph is a graph where each node connects to its k-nearest neighbors. We used a ring graph where each node connects to exactly 4 nearest neighbors. The eigenvectors are similar to the discrete cosine transform and the energy evenly spreads to each element in V [51]. Some properties of the ring graph are shown in Figure 1. For easier visualization, we only plot 20 nodes in Figure 1(a). In Figure 1(b), we show the degree distribution and see that it concentrates on 4, as expected. In Figure 1(c), we show the distribution of the leverage score of $\mathrm{V}_{(20)}$, which is the optimal sampling score when the SNR is large. Note that we set the bandwidth $K = 20$ to show the low-frequency band of the graph Fourier transform matrix. We see that the sampling scores are around 10^{-4}. This means that each node has the same probability to be chosen and uniform sampling is approximately the optimal sampling strategy.

Erdős-Rényi graph. An Erdős-Rényi graph is a random graph where each pair of nodes is connected with some probability [3]. We use a graph where each pair of nodes is connected with probability of 0.01, that is, each node has 100 neighbors on expectation. Some properties of the Erdős-Rényi graph are shown in Figure 2. For easier visualization, we only plot 100 nodes in Figure 1(a). In Figure 1(b), we show the degree distribution and we see that all the degrees are around 100. In Figure 1(c), we show the distribution of the leverage score of $\mathrm{V}_{(20)}$, which is the optimal sampling score when the SNR is large. We see that all the sampling scores are around 10^{-4}. Similarly to the ring graph, each node of the Erdős-Rényi graph has the similar probability to be chosen and uniform sampling is approximately the optimal sampling strategy.

Random geometric graph. A random geometric graph is a spatial graph where each of the nodes is assigned random coordinates in the box $[0, 1]^d$ and an edge appears when the distance between two nodes is in a given range [52]. We used a graph lying in the box $[0, 1]^2$, and two nodes are connected when the Euclidean distance is less than 0.03. Some properties of the random geometric graph are shown in Figure 3. In Figure 1(b), we show the degree distribution and we see that all the degrees are around 30. This matches the previous theory that given proper parameters, the degree distribution of a random geometric graph is the same as an Erdős-Rényi graph [52]. In Figure 2(c), we show the distribution of the leverage score of $\mathrm{V}_{(20)}$, which is the optimal sampling score when the SNR is large. We see that the distribution of the sampling scores is skewed. This means that even though all nodes have more or fewer degrees, a few nodes are much more important than the other nodes during sampling. In [52], the authors show that the cluster properties are different between a random geometric graph and an Erdős-Rényi graph. The proposed sampling scores capture these cluster properties through decomposing the graph adjacency matrix.

Small-world graph. A small-world graph is a graph where most nodes are not neighbors of one another, but can be reached from any other node by a small number of hops (steps) [2], [3]. It is well known that many real-world graphs, including social networks, the connectivity of the Internet, and gene networks show small-world graph characteristics. We use a graph generated from the WattsStrogatz model, where a ring graph is first built and the edges are rewired with probability 0.01%. Some properties of the small-world graph are shown in Figure 3. In Figure 1(b), we show the degree distribution and see that most degrees are around 2. A few nodes have 6 neighobors because of rewiring. In Figure 2(c), we show the distribution of the leverage score of $\mathrm{V}_{(20)}$, which is the optimal sampling score when the SNR is large. We see that the distribution of the sampling scores is skewed. Similarly to the random geometric graph, a few nodes have much higher probabilities to be chosen.

Power-law graph. A power-law graph is a graph where the more connected a node is, the more likely it is to receive new links, known as a preferential attachment graph [2], [3]. It is well known that the degree distribution of a preferential attachment graph follows the power law. We use a graph generated from the Barabási-Albert model, where new nodes are added to the network one at a time. Each new node is connected to one existing node with a probability that is proportional to the number of links that the existing nodes already have. Some properties of the power-law graph are shown in Figure 3. In Figure 1(b), we show the degree distribution and see that it is skewed, which clearly follows the power law. In Figure 2(c), we show the distribution of the leverage score of $\mathrm{V}_{(20)}$, which is the optimal sampling score when the SNR is large. We see that the distribution of the sampling scores is also skewed. Similarly to the random geometric graph and the small-world graph, a few nodes have much higher probabilities to be chosen.

Types. Based on our observation on the graph Fourier transform matrices of each graph, the ring graph and the Erdős-Rényi graph approximately satisfy the requirement to be the type-1 graph, and the random geometric graph, the small-world graph, the power-law graph approximately satisfy the requirement to be the type-2 graph. We thus expect that the experimentally designed sampling has similar performance with uniform sampling for the ring graph and the Erdős-Rényi graph, and that the experimentally designed sampling outperforms uniform sampling for the random geometric graph, the small-world graph, the power-law graph.

B. Simulated Graph Signals

For each graph A, we generate 1,000 graph signals by the following two steps: We first generate the graph frequency components as

$$\widehat{x}_k \begin{cases} \sim \mathcal{N}(1, 0.5^2) & \text{when } k < K; \\ = K^{2\beta}/k^{2\beta} & \text{when } k \geq K. \end{cases} \tag{11}$$

We then normalize $\widehat{\mathbf{x}}$ to have norm one, and obtain $\mathbf{x} = \mathrm{V}\,\widehat{\mathbf{x}}$. It is clear that $\mathbf{x} \in \mathrm{ABL}_{\mathrm{A}}(K, \beta, \mu)$, where $K = 10$ and β varies as 0.5 and 1. During sampling, we simulate the

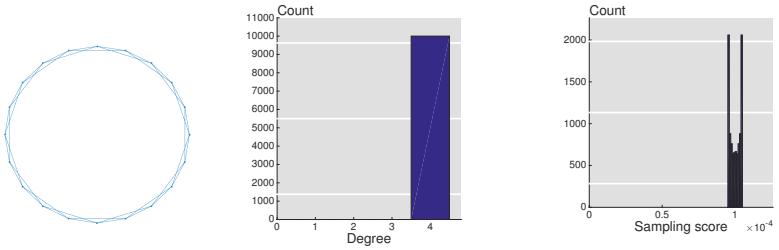

(a) Graph plot. (b) Histogram of degree. (c) Histogram of leverage score.

Fig. 1: Properties of the ring graph.

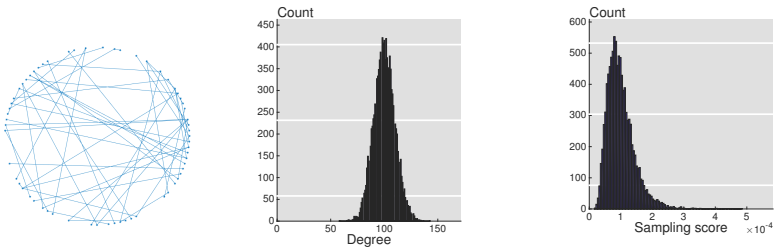

(a) Graph plot. (b) Histogram of degree. (c) Histogram of leverage score.

Fig. 2: Properties of the Erdős-Rényi graph.

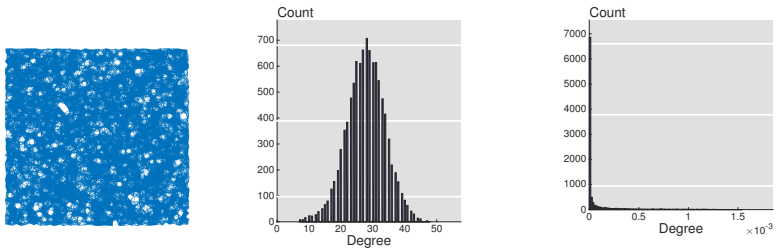

(a) Graph plot. (b) Histogram of degree. (c) Histogram of leverage score.

Fig. 3: Properties of the random geometric graph.

noise $\epsilon \sim \mathcal{N}(0, \sigma^2)$ and vary σ^2 from low noise level 10^{-4} ($\|\epsilon\|_2 / \|\mathbf{x}\|_2 = 1\%$) to high noise level 0.02 ($\|\epsilon\|_2 / \|\mathbf{x}\|_2 = 200\%$). In the recovery, we vary the sample size m from $1,000$ to $20,000$ and we set the bandwidth $K = \max(10, m^{1/2\beta+1})$ as suggested in Corollaries 4 and 6.

C. Results

We compare four sampling strategies, including uniform sampling (in blue), leverage score based sampling (in orange), square root of the leverage score based sampling (in purple), and degree based sampling (in red). Leverage score based sampling is approximately the optimal sampling scores when the SNR is large, square root of the leverage score based sampling is approximately the optimal sampling scores when the SNR is small. We also use the degree as the sampling scores because previous works show that the largest eigenvectors of adjacency matrices often have most of their mass localized on high-degree nodes [53], [54], which implies the high correlation between degree and leverage score. We evaluate the recovery performance by using the MSE,

$$\text{MSE} \;=\; \|\mathbf{x}^* - \mathbf{x}\|_2^2 \,,$$

where $\mathbf{x}^*$ is the recovered graph signal and $\mathbf{x}$ is the original graph signal. The simulation results for the ring graph, the Erdős-Rényi graph, the random geometric graph, the small-world graph, the power-law graph are shown in Figures 6, 7, 8, 9 and 10, respectively. We summarize the important points as follows.

- All of the sampling strategies perform similarly on the ring graph and the Erdős-Rényi graph, which matches Corollary 4.
- Experimentally designed sampling outperforms uniform sampling on the random geometric graph, the small-world graph and the power-law graph, which matches Corollary 6. Especially for the small-world graph, the power-law graph, uniform sampling is much worse than experimentally designed sampling.
- Leverage score based sampling outperforms all other sampling strategies when the noise level is low.

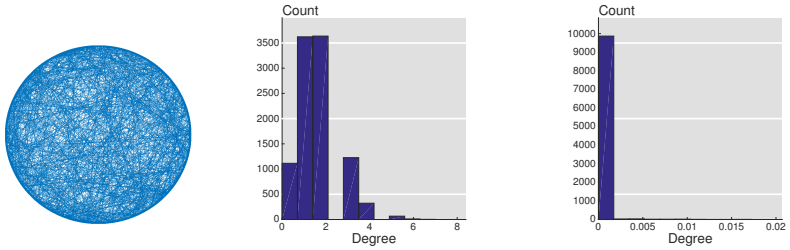

(a) Graph plot. (b) Histogram of degree. (c) Histogram of leverage score.

Fig. 4: Properties of the small-world graph.

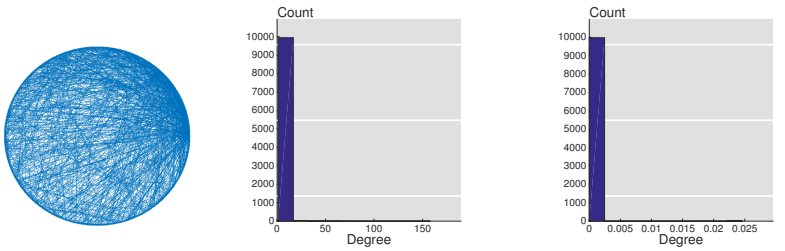

(a) Graph plot. (b) Histogram of degree. (c) Histogram of leverage score.

Fig. 5: Properties of the power-law graph.

- Square root of the leverage score based sampling outperforms all other sampling strategies when the noise level is high.
- Degree based sampling performs better than uniform sampling because of its correlation to the leverage score based sampling, but for the small-world graph, degree based sampling is still much worse than leverage score based sampling.
- When β is larger, the recovery performance is better because less energy exists in the high-frequency band of approximately bandlimited graph signals.
- When σ^2 is smaller, the recovery performance is better because of less noise.
- Comparing the Erdős-Rényi graph with the random geometric graph, the degree distribution may not show the property of a graph and the proposed sampling scores work as a reliable indicator of when experimentally designed sampling outperforms uniform sampling.

D. Discussion

The degree distribution does not tell everything about the graph structure. Degree only consider the information about neighbors, which is limited. Many other patterns may be more meaningful, such as clusters. Graph Fourier transform matrix is useful for understanding the graph structure. Here, we compute sampling scores from the graph Fourier transform matrix, and find that the random geometric graph has local cluster patterns. We believe that the graph Fourier transform matrix can be useful to study graph structure in many other cases.

Experimentally designed sampling is useful for semi-supervised learning with graphs. Many algorithms for semi-supervised learning are based on graphs that are constructed from a given dataset [55]. The graph is often constructed by modeling each node as a data sample and connecting two nodes by an edge if the distance between their features is in a given range, which is similar to the construction of random geometric graphs. Many structure-adaptive algorithms are proposed to find anchor points on graphs, which is essentially equivalent to experimentally designed sampling in this paper [56], [57]. In other words, many works use experimentally designed sampling implicitly without fully studying when and why experimentally designed sampling works. This paper provides a comprehensive explanation.

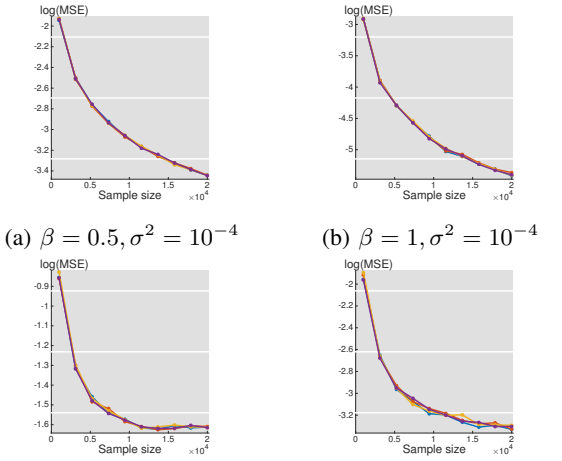

(a) $\beta = 0.5, \sigma^2 = 10^{-4}$ (b) $\beta = 1, \sigma^2 = 10^{-4}$

(d) $\beta = 0.5, \sigma^2 = 2 \times 10^{-2}$ (e) $\beta = 1, \sigma^2 = 2 \times 10^{-2}$

Fig. 6: MSE comparison for the ring graph for uniform sampling (in blue), leverage score based sampling (in orange), square root of the leverage score based sampling (in purple) and degree based sampling (in red).

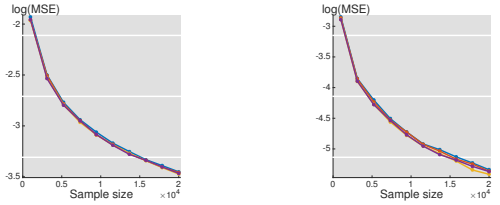

(a) $\beta = 0.5, \sigma^2 = 10^{-4}$. (b) $\beta = 1, \sigma^2 = 10^{-4}$.

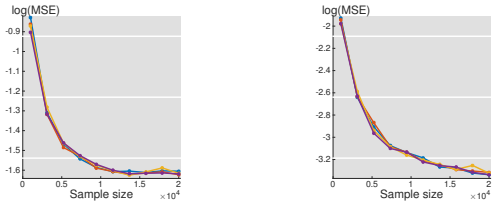

(c) $\beta = 0.5, \sigma^2 = 2 \times 10^{-2}$. (d) $\beta = 1, \sigma^2 = 2 \times 10^{-2}$.

Fig. 7: MSE comparison for the Erdős-Rényi graph for uniform sampling (in blue), leverage score based sampling (in orange), square root of the leverage score based sampling (in purple) and degree based sampling (in red).

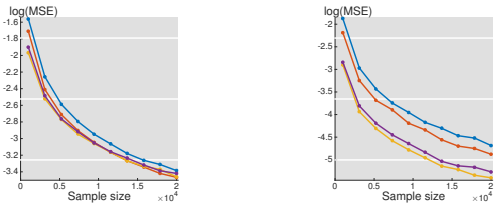

(a) $\beta = 0.5, \sigma^2 = 10^{-4}$. (b) $\beta = 1, \sigma^2 = 10^{-4}$.

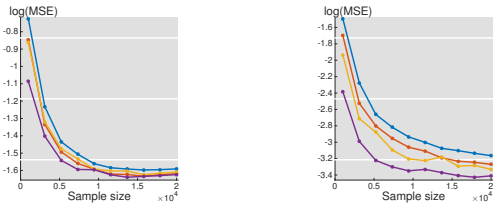

(c) $\beta = 0.5, \sigma^2 = 2 \times 10^{-2}$. (d) $\beta = 1, \sigma^2 = 2 \times 10^{-2}$.

Fig. 8: MSE comparison for the random geometric graph for uniform sampling (in blue), leverage score based sampling (in orange), square root of the leverage score based sampling (in purple) and degree based sampling (in red).

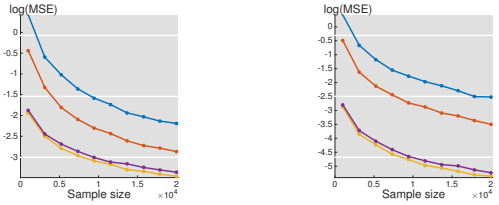

(a) $\beta = 0.5, \sigma^2 = 10^{-4}$. (b) $\beta = 1, \sigma^2 = 10^{-4}$.

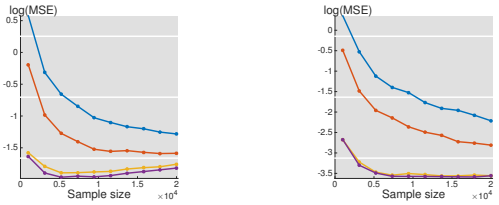

(c) $\beta = 0.5, \sigma^2 = 2 \times 10^{-2}$. (d) $\beta = 1, \sigma^2 = 2 \times 10^{-2}$.

Fig. 9: MSE comparison for the small-world graph for uniform sampling (in blue), leverage score based sampling (in orange), square root of the leverage score based sampling (in purple) and degree based sampling (in red).

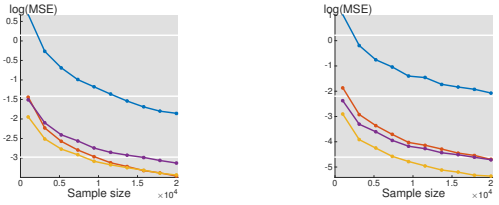

(a) $\beta = 0.5, \sigma^2 = 10^{-4}$. (b) $\beta = 1, \sigma^2 = 10^{-4}$.

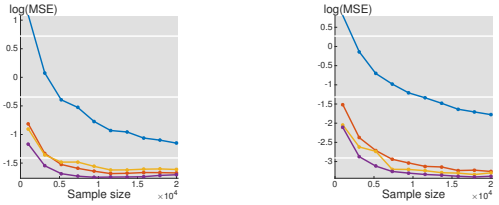

(c) $\beta = 0.5, \sigma^2 = 2 \times 10^{-2}$. (d) $\beta = 1, \sigma^2 = 2 \times 10^{-2}$.

Fig. 10: MSE comparison for the power-law graph for uniform sampling (in blue), leverage score based sampling (in orange), square root of the leverage score based sampling (in purple) and degree based sampling (in red).

VIII. Conclusions

We build a theoretical foundation for the recovery of smooth graph signals under uniform sampling, experimentally designed sampling, and active sampling. We propose a new class of approximately bandlimited graph signals that generalizes the class of the class of bandlimited graph signals. We show that experimentally designed sampling and active sampling have the same fundamental limitations, and can outperform uniform sampling on irregular graphs. We propose a recovery strategy with the analysis of its statistical properties. We show that the proposed recovery strategy attains the optimal rates of convergence on two specific types of graphs. To validate the recovery strategies, we test them on five specific graphs: a ring graph with k nearest neighbors, an Erdős-Rényi graph, a random geometric graph, a small-world graph, and a power-law graph and show that experimental results match the proposed theory well. This work gives a comprehensive explanation for why experimentally designed sampling works for semi-supervised learning with graph and shows the critical role of the graph Fourier transform matrix in analyzing graph structures.

References

[1] S. Chen, R. Varma, A. Singh, and J. Kovačević, "Signal recovery on graphs: Random versus experimentally designed sampling," in *Proc. Sampling Theory Appl.*, Washington, DC, May 2015, pp. 337–341.

[2] M. Jackson, *Social and Economic Networks*, Princeton University Press, 2008.

[3] M. Newman, *Networks: An Introduction*, Oxford University Press, 2010.

[4] D. I. Shuman, S. K. Narang, P. Frossard, A. Ortega, and P. Vandergheynst, "The emerging field of signal processing on graphs: Extending high-dimensional data analysis to networks and other irregular domains," *IEEE Signal Process. Mag.*, vol. 30, pp. 83–98, May 2013.

[5] A. Sandryhaila and J. M. F. Moura, "Big data processing with signal processing on graphs," *IEEE Signal Process. Mag.*, vol. 31, no. 5, pp. 80–90, 2014.

[6] S. Chen, R. Varma, A. Sandryhaila, and J. Kovačević, "Discrete signal processing on graphs: Sampling theory," *IEEE Trans. Signal Process.*, vol. 63, pp. 6510 – 6523, Aug. 2015.

[7] A. Anis, A. Gadde, and A. Ortega, "Efficient sampling set selection for bandlimited graph signals using graph spectral proxies," *IEEE Trans. Signal Process.*, 2015, Submitted.

[8] X. Wang, P. Liu, and Y. Gu, "Local-set-based graph signal reconstruction," *IEEE Trans. Signal Process.*, vol. 63, no. 9, May 2015.

[9] S. Chen, A. Sandryhaila, J. M. F. Moura, and J. Kovačević, "Signal recovery on graphs: Variation minimization," *IEEE Trans. Signal Process.*, vol. 63, no. 17, pp. 4609–4624, Sept. 2015.

[10] S. K. Narang, Akshay Gadde, and Antonio Ortega, "Signal processing techniques for interpolation in graph structured data," in *Proc. IEEE Int. Conf. Acoust., Speech, Signal Process.*, Vancouver, May 2013, pp. 5445–5449.

[11] X. Zhu and M. Rabbat, "Approximating signals supported on graphs," in *Proc. IEEE Int. Conf. Acoust., Speech, Signal Process.*, Kyoto, Japan, Mar. 2012, pp. 3921 – 3924.

[12] S. Chen, R. Varma, A. Singh, and J. Kovačević, "Signal representations on graphs: Tools and applications," *arXiv:1512.05406*, 2015.

[13] A. Agaskar and Y. M. Lu, "A spectral graph uncertainty principle," *IEEE Trans. Inf. Theory*, vol. 59, no. 7, pp. 4338–4356, July 2013.

[14] M. Tsitsvero, S. Barbarossa, and P. D. Lorenzo, "Signals on graphs: Uncertainty principle and sampling," *arXiv:1507.08822*, 2015.

[15] D. Thanou, D. I. Shuman, and P. Frossard, "Learning parametric dictionaries for signals on graphs," *IEEE Trans. Signal Process.*, vol. 62, pp. 3849–3862, June 2014.

[16] S. Chen, F. Cerda, P. Rizzo, J. Bielak, J. H. Garrett, and J. Kovačević, "Semi-supervised multiresolution classification using adaptive graph filtering with application to indirect bridge structural health monitoring," *IEEE Trans. Signal Process.*, vol. 62, no. 11, pp. 2879–2893, June 2014.

[17] V. N. Ekambaram, B. Ayazifar G. Fanti, and K. Ramchandran, "Wavelet-regularized graph semi-supervised learning," in *Proc. IEEE Glob. Conf. Signal Information Process.*, Austin, TX, Dec. 2013, pp. 423–426.

[18] S. K. Narang and A. Ortega, "Perfect reconstruction two-channel wavelet filter banks for graph structured data," *IEEE Trans. Signal Process.*, vol. 60, pp. 2786–2799, June 2012.

[19] S. Chen, A. Sandryhaila, J. M. F. Moura, and J. Kovačević, "Signal denoising on graphs via graph filtering," in *Proc. IEEE Glob. Conf. Signal Information Process.*, Atlanta, GA, Dec. 2014, pp. 872–876.

[20] N. Tremblay and P. Borgnat, "Graph wavelets for multiscale community mining," *IEEE Trans. Signal Process.*, vol. 62, pp. 5227–5239, Oct. 2014.

[21] X. Dong, P. Frossard, P. Vandergheynst, and N. Nefedov, "Clustering on multi-layer graphs via subspace analysis on Grassmann manifolds," *IEEE Trans. Signal Process.*, vol. 62, no. 4, pp. 905–918, Feb. 2014.

[22] P.-Y. Chen and A.O. Hero, "Local Fiedler vector centrality for detection of deep and overlapping communities in networks," in *Proc. IEEE Int. Conf. Acoust., Speech, Signal Process.*, Florence, 2014, pp. 1120–1124.

[23] S. K. Narang and Antonio Ortega, "Compact support biorthogonal wavelet filterbanks for arbitrary undirected graphs," *IEEE Trans. Signal Process.*, vol. 61, no. 19, pp. 4673–4685, Oct. 2013.

[24] A. Sandryhaila and J. M. F. Moura, "Discrete signal processing on graphs," *IEEE Trans. Signal Process.*, vol. 61, no. 7, pp. 1644–1656, Apr. 2013.

[25] D. K. Hammond, P. Vandergheynst, and R. Gribonval, "Wavelets on graphs via spectral graph theory," *Appl. Comput. Harmon. Anal.*, vol. 30, pp. 129–150, Mar. 2011.

[26] S.l K. Narang, G. Shen, and A. Ortega, "Unidirectional graph-based wavelet transforms for efficient data gathering in sensor networks," in *Proc. IEEE Int. Conf. Acoust., Speech, Signal Process.*, Dallas, TX, Mar. 2010, pp. 2902–2905.

[27] M. Vetterli, J. Kovačević, and V. K. Goyal, *Foundations of Signal Processing*, Cambridge University Press, Cambridge, 2014, http://www.fourierandwavelets.org/.

[28] J. Kovačević and M. Püschel, "Algebraic signal processing theory: Sampling for infinite and finite 1-D space," *IEEE Trans. Signal Process.*, vol. 58, no. 1, pp. 242–257, Jan. 2010.

[29] M. Vetterli, P. Marziliano, and T. Blu, "Sampling signals with finite rate of innovation," *IEEE Trans. Signal Process.*, vol. 50, no. 6, pp. 1417–1428, June 2002.

[30] P. L. Dragotti, M. Vetterli, and T. Blu, "Sampling moments and reconstructing signals of finite rate of innovation: Shannon meets Strang-Fix," *IEEE Trans. Signal Process.*, vol. 55, 2007.

[31] E. J. Candés, J. K. Romberg, and T. Tao, "Stable signal recovery from incomplete and inaccurate measurements," *Commun. Pure Appl. Math.*, vol. 59, pp. 1207–1223, Aug. 2006.

[32] E. J. Candès, Y. Eldar, D. Needell, and P. Randall, "Compressed sensing with coherent and redundant dictionaries," *Applied and Computational Harmonic Analysis*, vol. 31, pp. 59–73, 2010.

[33] Y. M. Lu and M. N. Do, "Sampling signals from a union of subspaces," *IEEE Signal Process. Mag.*, vol. 25, no. 2, pp. 41–47, Mar. 2008.

[34] T. Blumensath and M. E. Davies, "Sampling theorems for signals from the union of finite-dimensional linear subspaces," *IEEE Trans. Inf. Theory*, vol. 55, pp. 1872–1882, Apr. 2009.

[35] I. Z. Pesenson, "Sampling in Paley-Wiener spaces on combinatorial graphs," *Trans. Am. Math. Soc.*, vol. 360, no. 10, pp. 5603–5627, May 2008.

[36] X. Zhu and M. Rabbat, "Graph spectral compressed sensing for sensor networks," in *Proc. IEEE Int. Conf. Acoust., Speech, Signal Process.*, Kyoto, Japan, Mar. 2012, pp. 2865 – 2868.

[37] A. Anis, A. Gadde, and A. Ortega, "Towards a sampling theorem for signals on arbitrary graphs," in *Proc. IEEE Int. Conf. Acoust., Speech, Signal Process.*, Florence, May 2014, pp. 3864–3868.

[38] S. Chen, A. Sandryhaila, and J. Kovačević, "Sampling theory for graph signals," in *Proc. IEEE Int. Conf. Acoust., Speech, Signal Process.*, Brisbane, Apr. 2015, pp. 3392 – 3396.

[39] X. Wang, M. Wang, and Y. Gu, "A distributed tracking algorithm for reconstruction of graph signals," *IEEE Journal of Selected Topics on Signal Processing*, vol. 9, no. 4, June 2015.

[40] S. Chen, A. Sandryhaila, and J. Kovačević, "Distributed algorithm for graph signal inpainting," in *Proc. IEEE Int. Conf. Acoust., Speech, Signal Process.*, Brisbane, Apr. 2015, pp. 3731 – 3735.

[41] X. Wang, J. Chen, and Y. Gu, "Local measurement and reconstruction for noisy graph signals," *arXiv:1504.01456*, 2015.

[42] A. G. Marques, S. Segarra, G. Leus, and A. Ribeiro, "Sampling of graph signals with successive local aggregations," *IEEE Trans. Signal Process.*, Dec 2015.

[43] S. Segarra, A. G. Marques, G. Leus, and A. Ribeiro, "Reconstruction of graph signals through percolation from seeding nodes," *IEEE Trans. Signal Process.*, 2015, Submitted.

[44] R. Castro, R. Willett, and R. Nowak, "Faster rates in regression via active learning," in *Proc. Neural Information Process. Syst.*, Vancouver, Dec. 2005.

[45] R. Castro and R. Nowak, "Minimax bounds for active learning," *IEEE Trans. Inf. Theory*, vol. 54, no. 5, pp. 2339–2353, July 2008.

[46] A. P. Korostelev and A. B. Tsybakov, *Minimax theory of image reconstruction*, Lecture Notes on Statistics. Springer, 1993.

[47] A. Sandryhaila and J. M. F. Moura, "Discrete signal processing on graphs: Frequency analysis," *IEEE Trans. Signal Process.*, vol. 62, no. 12, pp. 3042–3054, June 2014.

[48] J. Sharpnack and A. Singh, "Identifying graph-structured activation patterns in networks," in *Proc. Neural Information Process. Syst.*, Vancouver, Dec. 2010, pp. 2137–2145.

[49] I. M. Johnstone, *Minimax Bayes, Asymptotic Minimax and Sparse Wavelet Priors*, Statistical Decision Theory and Related Topics V. Springer, 1994.

[50] P. Ma, M. W. Mahoney, and B. Yu, "A statistical perspective on algorithmic leveraging," *J. Mach. Learn. Res.*, vol. 16, pp. 861–911, 2015.

[51] A. Sandryhaila, J. Kovačević, and M. Püschel, "Algebraic signal processing theory: 1-D nearest-neighbor models," *IEEE Trans. Signal Process.*, vol. 60, no. 5, pp. 2247–2259, May 2012.

[52] J. Dall and M. Christensen, "Random geometric graphs," *Phys. Rev. E*, vol. 66, July 2002.

[53] K. I. Goh, B. Kahng, and D. Kim, "Spectra and eigenvectors of scale-free networks," *Phys Rev E*, vol. 64, no. 5, Nov. 2001.

[54] M. Cucuringu and M. W. Mahoney, "Localization on low-order eigenvectors of data matrices," *Technical Report, Preprint: arXiv:1109.1355*, 2011.

[55] X. Zhu, "Semi-supervised learning literature survey," Tech. Rep. 1530, University Wisconsin-Madison, 2005.

[56] Q. Gu and J. Han, "Towards active learning on graphs: An error bound minimization approach," in *Proc. IEEE Int. Conf. Data Mining*, Brussels, Dec. 2012, pp. 882 – 887.

[57] A. Gadde, A. Anis, and A. Ortega, "Active semi-supervised learning using sampling theory for graph signals," in *KDD*, New York, New York, USA, 2014, pp. 492–501.

APPENDIX

A. Proof of Theorem 3

We aim to construct a typical set of vectors in $\mathcal{F}$, and use the Fano's method. Let $\mathbf{v}_k$ be the kth column of V, $\mathbf{v}^{(i)}$ be the ith row of V, $\mathcal{X}$ be a pruned hypercube and

$$\mathcal{F}' = \{\mathbf{x}^{(\mathbf{w})} = \mathrm{V}\,\widehat{\mathbf{x}} \odot \mathbf{w} = \sum_{k=\kappa_0}^{2\kappa_0-1} w_k \psi_k, \quad \mathbf{w} \in \mathcal{X}\},$$

where κ_0 is no smaller than the bandwidth K,

$$\psi_k = \widehat{x}_k \mathbf{v}_k = (\pm)^k \sqrt{\frac{c\mu \left\|\mathbf{x}\right\|_2^2}{\kappa_0(1+k^{2\beta})}} \mathbf{v}_k,$$

and $0 < c < 1$. It is easy to check that $\mathcal{F}' \subseteq \mathcal{F}$. Let $d(\mathbf{x}, \mathbf{y}) = \left\|\mathbf{x} - \mathbf{y}\right\|_2$; we thus have

$$\begin{aligned} d^2(\mathbf{x}^{(\mathbf{w})}, \mathbf{x}^{(\mathbf{u})}) &= \left\|\mathrm{V}\,\widehat{\mathbf{x}} \odot (\mathbf{w}-\mathbf{u})^2\right\|_2^2 \\ &= \sum_{k=\kappa_0}^{2\kappa_0-1} (w_k - u_k)^2 \widehat{x}_k^2 \\ &= \sum_{k=\kappa_0}^{2\kappa_0-1} (w_k - u_k)^2 \frac{c\mu \left\|\mathbf{x}\right\|_2^2}{\kappa_0(1+k^{2\beta})} \\ &\overset{(a)}{\geq} \sum_{k=\kappa_0}^{2\kappa_0-1} (w_k - u_k)^2 \cdot \frac{c\mu \left\|\mathbf{x}\right\|_2^2}{\kappa_0(1+(2\kappa_0)^{2\beta})} \\ &\overset{(b)}{\geq} \frac{\kappa_0}{8} \cdot \frac{c\mu \left\|\mathbf{x}\right\|_2^2}{\kappa_0(1+(2\kappa_0)^{2\beta})} \;\geq\; c_1 \mu \kappa_0^{-2\beta} \left\|\mathbf{x}\right\|_2^2, \end{aligned}$$

where (a) follows from $k \leq 2K$, and (b) from the Varshamov-Gilbert lemma. To use the Fanno's method, we need to bound the Kullback-Leibler divergence,

$$\begin{aligned} & KL(p_{\mathbf{w}}, p_{\mathbf{w}_0}|\mathcal{M}) \\ = & \sum_{i\in\mathcal{M}} \mathbb{E}_{\mathbf{w}} \left[\log \frac{p(y_i - x_i^{(\mathbf{w})})}{p(y_i - x_i^{(\mathbf{w}_0)})}\right] \\ \leq & \sum_{i\in\mathcal{M}} \left[\frac{1}{2\sigma^2}(x_i^{(\mathbf{w})} - x_i^{(\mathbf{w}_0)})^2\right] \\ = & \sum_{i\in\mathcal{M}} \left[\frac{1}{2\sigma^2}\left(\mathbf{v}^{(i)*}(\widehat{\mathbf{x}} \odot \mathbf{w})\right)^2\right] \\ = & \frac{1}{2\sigma^2} \sum_{i\in\mathcal{M}} \left(\sum_{k=\kappa_0}^{2\kappa_0-1} \widehat{x}_k w_k \mathrm{V}_{ik}\right)^2 \\ = & \frac{1}{2\sigma^2} \sum_{i\in\mathcal{M}} \Bigg(\sum_{k=\kappa_0}^{2\kappa_0-1} (\widehat{x}_k w_k \mathrm{V}_{ik})^2 \\ & + \sum_{k,k'=\kappa_0, k\neq k'}^{2\kappa_0-1} \widehat{x}_k \widehat{x}_{k'} w_k w_{k'} \mathrm{V}_{ik} \mathrm{V}_{ik'} \Bigg) \\ \leq & \frac{1}{2\sigma^2} \sum_{i\in\mathcal{M}} \Bigg(\sum_{k=\kappa_0}^{2\kappa_0-1} \frac{c\mu \left\|\mathbf{x}\right\|_2^2 w_k^2 \mathrm{V}_{ik}^2}{2\kappa_0(1+k^{2\beta})} \\ & + \sum_{k,k'=\kappa_0, k\neq k'}^{2\kappa_0-1} (-1)^{k+k'} \frac{c\mu \left\|\mathbf{x}\right\|_2^2 w_k w_{k'} \mathrm{V}_{ik} \mathrm{V}_{ik'}}{\kappa_0 \sqrt{1+k^{2\beta}} \sqrt{1+k'^{2\beta}}} \Bigg) \\ \leq & \frac{c'\mu \left\|\mathbf{x}\right\|_2^2}{\sigma^2} \sum_{i\in\mathcal{M}} \sum_{k=\kappa_0}^{2\kappa_0-1} \frac{\mathrm{V}_{ik}^2}{\kappa_0(1+\kappa_0^{2\beta})} + \delta \\ \asymp & \frac{c'\mu \left\|\mathbf{x}\right\|_2^2}{\sigma^2} \kappa_0^{-(2\beta+1)} \sum_{i\in\mathcal{M}} \sum_{k=\kappa_0}^{2\kappa_0-1} \mathrm{V}_{ik}^2, \end{aligned}$$

where $\delta = \sum_{k,k'=\kappa_0, k\neq k'}^{2\kappa_0-1} (-1)^{k+k'} \frac{c\mu \left\|\mathbf{x}\right\|_2^2 w_k w_{k'} \mathrm{V}_{ik} \mathrm{V}_{ik'}}{\kappa_0 \sqrt{1+k^{2\beta}} \sqrt{1+k'^{2\beta}}}$ is small because of the cross signs. For uniform sampling, the sampling set $\mathcal{M}$ is chosen randomly, thus, we have

$$\begin{aligned} & KL(p_{\mathbf{w}}, p_{\mathbf{w}_0}) \\ = & \mathbb{E}_{\mathcal{M}}\left[KL(p_{\mathbf{w}}, p_{\mathbf{w}_0}|\mathcal{M})\right] \\ \leq & \frac{c\mu \left\|\mathbf{x}\right\|_2^2}{\sigma^2} \kappa_0^{-(2\beta+1)} \mathbb{E}_{\mathcal{M}} \left(\sum_{i\in\mathcal{M}} \sum_{k=\kappa_0}^{2\kappa_0-1} \mathrm{V}_{ik}^2\right) \\ \overset{(a)}{=} & \frac{c\mu \left\|\mathbf{x}\right\|_2^2}{\sigma^2} K^{-(2\beta+1)} \mathbb{E}_i \left(m \sum_{k=\kappa_0}^{2\kappa_0-1} \mathrm{V}_{ik}^2\right) \\ = & \frac{c\mu \left\|\mathbf{x}\right\|_2^2}{\sigma^2} K^{-(2\beta+1)} m \sum_{j=1}^{N} \sum_{k=\kappa_0}^{2\kappa_0-1} \mathrm{V}_{jk}^2 \, \mathbb{P}(j=i) \\ = & \frac{c\mu \left\|\mathbf{x}\right\|_2^2}{\sigma^2} \kappa_0^{-(2\beta+1)} \frac{m}{N} \sum_{j=1}^{N} \sum_{k=\kappa_0}^{2\kappa_0-1} \mathrm{V}_{jk}^2 \\ \leq & \frac{c\mu \left\|\mathbf{x}\right\|_2^2}{\sigma^2 \kappa_0^{2\beta+1} N} \left\|\mathrm{V}_{(2,\kappa_0)}\right\|_F^2 m, \end{aligned}$$

where (a) follows from the independence of each sample, $\mathbb{P}(j=i)$ denotes the probability to sample the ith node that equals j, and $\left\|\mathrm{V}_{(2,\kappa_0)}\right\|_F^2 = \sum_{j=1}^{N} \sum_{k=\kappa_0}^{2\kappa_0-1} \mathrm{V}_{jk}^2$.

For experimentally designed sampling, we can choose the sampling set $\mathcal{M}$ to maximize $\sum_{i\in\mathcal{M}} \sum_{k=\kappa_0}^{2\kappa_0-1} \mathrm{V}_{ik}^2$; we thus have

$$\begin{aligned} KL(p_{\mathbf{w}}, p_{\mathbf{w}_0}) &\leq \frac{c\mu \left\|\mathbf{x}\right\|_2^2}{\sigma^2} \kappa_0^{-(2\beta+1)} \max_{\mathcal{M}} \sum_{i\in\mathcal{M}} \sum_{k=\kappa_0}^{2\kappa_0-1} \mathrm{V}_{ik}^2 \\ &\leq \frac{c\mu \left\|\mathbf{x}\right\|_2^2}{\sigma^2} \kappa_0^{-(2\beta+1)} \left\|\mathrm{V}_{(2,\kappa_0)}\right\|_{2,\infty}^2 m. \end{aligned}$$

For active sampling, we cannot get more benefit from signal coefficients, so the KL divergence is the same of the experimentally designed sampling.r By Fanno's lemma, we finally have the lower bounds for three sampling strategies. ■

B. Proof of Theorem 4

We aim to bound the MSE by splitting to a bias term and a variance term.

$$\begin{aligned} & \mathbb{E}\left\|\mathbf{x}^* - \mathbf{x}\right\|_2^2 \\ = & \mathbb{E}\left\|\mathbf{x}^* - \mathbf{x}\right\|_2^2 \\ = & \mathbb{E}\left\|\mathbf{x}^* - \mathbb{E}\mathbf{x}^* + \mathbb{E}\mathbf{x}^* - \mathbf{x}\right\|_2^2 \\ = & \mathbb{E}\left(\left\|\mathbf{x}^* - \mathbb{E}\mathbf{x}^*\right\|_2^2 + \left\|\mathbb{E}\mathbf{x}^* - \mathbf{x}\right\|_2^2 + 2(\mathbf{x}^* - \mathbb{E}\mathbf{x}^*)^T(\mathbb{E}\mathbf{x}^* - \mathbf{x})\right) \\ = & \left\|\mathbb{E}\mathbf{x}^* - \mathbf{x}\right\|_2^2 + \mathbb{E}\left\|\mathbf{x}^* - \mathbb{E}\mathbf{x}^*\right\|_2^2, \end{aligned}$$

where the first term is bias and the second term is variance. For each element in the bias term, we have

$$\begin{aligned}
\mathbb{E}x_i^* &= \sum_{k<\kappa} \mathrm{V}_{ik}\, \mathbb{E}_{\mathcal{M},\epsilon}\left(\sum_{\mathcal{M}_j\in\mathcal{M}} \mathrm{U}_{k\mathcal{M}_j}\, \mathrm{W}_{\mathcal{M}_j,\mathcal{M}_j}(x_{\mathcal{M}_j}+\epsilon_{\mathcal{M}_j})\right)\\
&\overset{(a)}{=} \sum_{k<\kappa} \mathrm{V}_{ik}\, m\mathbb{E}_\ell\left(\mathrm{U}_{k\ell}\,\frac{1}{m\pi_l}x_\ell\right)\\
&= \sum_{k<\kappa} \mathrm{V}_{ik}\, m\sum_{\ell=1}^{N}\left(\mathrm{U}_{k\ell}\,\frac{1}{m\pi_\ell}x_\ell\right)\pi_\ell\\
&= \sum_{k<\kappa} \mathrm{V}_{ik}\sum_{\ell=1}^{N}\mathrm{U}_{k\ell}\,x_\ell\\
&= \sum_{k<\kappa} \mathrm{V}_{ik}\,\widehat{x}_k,
\end{aligned}$$

where (a) follows from the independence of each sample. For all the elements, we have

$$\mathbb{E}\mathbf{x}^* = \mathrm{V}_{(\kappa)}\,\widehat{\mathbf{x}}_{(\kappa)},$$

which leads to Lemma 1.

We next bound the variance term by splitting into two parts, with and without noise. For each element in the variance term, we have

$$\begin{aligned}
&x_i^* - \mathbb{E}x_i^*\\
=\;& \sum_{k<\kappa} \mathrm{V}_{ik}\left(\sum_{\mathcal{M}_j\in\mathcal{M}} \mathrm{U}_{k\mathcal{M}_j}\,\mathrm{W}_{\mathcal{M}_j,\mathcal{M}_j}\,y_{\mathcal{M}_j}\right) - \sum_{k<\kappa}\mathrm{V}_{ik}\,\widehat{x}_k\\
=\;& \sum_{k<\kappa} \mathrm{V}_{ik}\sum_{\mathcal{M}_j\in\mathcal{M}} \mathrm{U}_{k\mathcal{M}_j}\,\mathrm{W}_{\mathcal{M}_j,\mathcal{M}_j}\,\epsilon_{\mathcal{M}_j}\\
&+\sum_{k<\kappa} \mathrm{V}_{ik}\left(\sum_{\mathcal{M}_j\in\mathcal{M}} \mathrm{U}_{k\mathcal{M}_j}\,\mathrm{W}_{\mathcal{M}_j,\mathcal{M}_j}\,x_{\mathcal{M}_j} - \widehat{x}_k\right)\\
=\;& \Delta_i^{(1)} + \Delta_i^{(2)},
\end{aligned}$$

where $\Delta^{(1)}$ is the variance from noise and $\Delta^{(2)}$ is the variance from sampling. To bound $\Delta_i^{(1)}$, we have

$$\begin{aligned}
&\mathbb{E}||\Delta_i^{(1)}||^2\\
=\;& \mathbb{E}\Bigg[\Bigg(\sum_{k<\kappa} \mathrm{V}_{ik}\sum_{\mathcal{M}_j\in\mathcal{M}} \mathrm{U}_{k\mathcal{M}_j}\,\mathrm{W}_{\mathcal{M}_j,\mathcal{M}_j}\,\epsilon_{\mathcal{M}_j}\Bigg)\\
&\Bigg(\sum_{k'<\kappa} \mathrm{V}_{ik'}\sum_{\mathcal{M}_{j'}\in\mathcal{M}} \mathrm{U}_{k'\mathcal{M}_{j'}}\,\mathrm{W}_{\mathcal{M}_{j'},\mathcal{M}_{j'}}\,\epsilon_{\mathcal{M}_{j'}}\Bigg)\Bigg]\\
=\;& \mathbb{E}\Bigg(\sum_{k,k'<\kappa} \mathrm{V}_{ik}\,\mathrm{V}_{ik'}\sum_{\mathcal{M}_j,\mathcal{M}_{j'}\in\mathcal{M}} \mathrm{U}_{k\mathcal{M}_j}\\
&\mathrm{U}_{k'\mathcal{M}_{j'}}\,\mathrm{W}_{\mathcal{M}_j,\mathcal{M}_j}\,\mathrm{W}_{\mathcal{M}_{j'},\mathcal{M}_{j'}}\,\epsilon_{\mathcal{M}_j}\epsilon_{\mathcal{M}_{j'}}\Bigg)\\
=\;& \sum_{k,k'<\kappa} \mathrm{V}_{ik}\,\mathrm{V}_{ik'}\,m\mathbb{E}_{\ell,\epsilon}\left(\mathrm{U}_{k\ell}^2\,\frac{1}{m^2\pi_\ell^2}\epsilon_\ell^2\right)\\
=\;& \sum_{k,k'<\kappa} \mathrm{V}_{ik}\,\mathrm{V}_{ik'}\,m\sum_{\ell=1}^{N}\mathrm{U}_{k\ell}\,\mathrm{U}_{k'\ell}\,\frac{1}{m^2\pi_\ell^2}\mathbb{E}\epsilon_\ell^2\pi_\ell\\
=\;& \sigma^2\sum_{k,k'<\kappa} \mathrm{V}_{ik}\,\mathrm{V}_{ik'}\sum_{\ell=1}^{N}\frac{1}{m\pi_\ell}\,\mathrm{U}_{k\ell}\,\mathrm{U}_{k'\ell}\,.
\end{aligned}$$

To bound $\Delta_i^{(2)}$, we have

$$\begin{aligned}
&\mathbb{E}\left\|\Delta_i^{(2)}\right\|_2^2\\
=\;& \mathbb{E}\Bigg[\sum_{k<\kappa} \mathrm{V}_{ik}\left(\sum_{\mathcal{M}_j\in\mathcal{M}} \mathrm{U}_{k\mathcal{M}_j}\,\mathrm{W}_{\mathcal{M}_j,\mathcal{M}_j}\,x_{\mathcal{M}_j} - \widehat{x}_k\right)\\
&\sum_{k'<\kappa} \mathrm{V}_{ik'}\left(\sum_{\mathcal{M}_{j'}\in\mathcal{M}} \mathrm{U}_{k'\mathcal{M}_{j'}}\,\mathrm{W}_{\mathcal{M}_{j'},\mathcal{M}_{j'}}\,x_{\mathcal{M}_{j'}} - \widehat{x}_{k'}\right)\Bigg]\\
=\;& \mathbb{E}\Bigg[\sum_{k,k'<K} \mathrm{V}_{ik}\,\mathrm{V}_{ik'}\Bigg(\sum_{\mathcal{M}_j,\mathcal{M}_{j'}\in\mathcal{M}} \mathrm{U}_{k\mathcal{M}_j}\,\mathrm{U}_{k'\mathcal{M}_{j'}}\,\mathrm{W}_{\mathcal{M}_j,\mathcal{M}_j}\\
&\mathrm{W}_{\mathcal{M}_{j'},\mathcal{M}_{j'}}\,x_{\mathcal{M}_j}x_{\mathcal{M}_{j'}} - \widehat{x}_k\widehat{x}_{k'}\Bigg)\Bigg]\\
=\;& \sum_{k,k'<\kappa} \mathrm{V}_{ik}\,\mathrm{V}_{ik'}\Bigg[\mathbb{E}_{\mathcal{M}}\Bigg(\sum_{\mathcal{M}_j\neq\mathcal{M}_{j'},\mathcal{M}_j,\mathcal{M}_{j'}\in\mathcal{M}} \mathrm{U}_{k\mathcal{M}_j}\,\mathrm{U}_{k'\mathcal{M}_{j'}}\\
&x_{\mathcal{M}_j}x_{\mathcal{M}_{j'}}\Bigg) + \mathbb{E}_{\mathcal{M}}\Bigg(\sum_{\mathcal{M}_j=\mathcal{M}_{j'},\mathcal{M}_j,\mathcal{M}_{j'}\in\mathcal{M}} \mathrm{U}_{k\mathcal{M}_j}\,\mathrm{U}_{k'\mathcal{M}_{j'}}\\
&x_{\mathcal{M}_{j'}}x_{\mathcal{M}_{j'}}\Bigg) - \widehat{x}_k\widehat{x}_{k'}\Bigg]\\
=\;& \sum_{k,k'<\kappa} \mathrm{V}_{ik}\,\mathrm{V}_{ik'}\Bigg[(m^2-m)\mathbb{E}_{\ell,\ell'}\left(\frac{\mathrm{U}_{k\ell}\,\mathrm{U}_{k'\ell'}\,x_\ell x_{\ell'}}{m^2\pi_\ell\pi_{\ell'}}\right)\\
&+m\mathbb{E}_\ell\left(\frac{\mathrm{U}_{k\ell}\,\mathrm{U}_{k'\ell}\,x_\ell^2}{m^2\pi_\ell^2}\right) - \widehat{x}_k\widehat{x}_{k'}\Bigg]\\
=\;& \sum_{k,k'<\kappa} \mathrm{V}_{ik}\,\mathrm{V}_{ik'}\Bigg[(m^2-m)\sum_{\ell,\ell'=1}^{N}\frac{\mathrm{U}_{k\ell}\,\mathrm{U}_{k\ell'}\,x_\ell x_{\ell'}}{m^2\pi_\ell\pi_{\ell'}}\pi_\ell\pi_{\ell'}\\
&+m\sum_{\ell=1}^{N}\frac{\mathrm{U}_{k\ell}\,\mathrm{U}_{k'\ell}\,x_\ell^2}{m^2\pi_\ell^2}\pi_\ell - \widehat{x}_k\widehat{x}_{k'}\Bigg]\\
=\;& \sum_{k,k'<\kappa}\left(\mathrm{V}_{ik}\,\mathrm{V}_{ik'}\sum_{\ell=1}^{N}\mathrm{U}_{k\ell}\,\mathrm{U}_{k'\ell}\,\frac{x_\ell^2}{m\pi_\ell} - \frac{1}{m}\widehat{x}_k\widehat{x}_{k'}\right).
\end{aligned}$$

We combine the bounds for both $\Delta_i^{(1)}$ and $\Delta_i^{(2)}$, and obtain the bounds for the variance term,

$$\begin{aligned}
&\mathbb{E}\left\|\mathbf{x}^* - \mathbb{E}\mathbf{x}^*\right\|_2^2\\
=\;& \sum_{i=1}^{N}\mathbb{E}\left\|x_i^* - \mathbb{E}x_i^*\right\|\\
=\;& \sum_{i=1}^{N}\left(\mathbb{E}\left\|\Delta_i^{(1)}\right\|_2^2 + \mathbb{E}\left\|\Delta_i^{(2)}\right\|_2^2\right)\\
=\;& \sum_{i=1}^{N}\sum_{k,k'<\kappa} \mathrm{V}_{ik}\,\mathrm{V}_{ik'}\sum_{\ell=1}^{N}\mathrm{U}_{k\ell}\,\mathrm{U}_{k\ell'}\,\frac{\sigma^2+x_\ell^2}{m\pi_\ell} - \frac{1}{m}\sum_{k,k'<\kappa}\widehat{x}_k\widehat{x}_{k'}\\
=\;& \mathrm{Tr}\left(\mathrm{V}_{(\kappa)}\,\mathrm{U}_{(\kappa)}\,\mathrm{W}_C\,\mathrm{U}_{(\kappa)}^T\,\mathrm{V}_{(\kappa)}^T\right) - \frac{1}{m}\left\|\widehat{\mathbf{x}}_{(\kappa)}\right\|_2^2\\
=\;& \mathrm{Tr}\left(\mathrm{U}_{(\kappa)}\,\mathrm{W}_C\,\mathrm{V}_{(\kappa)}\right) - \frac{1}{m}\left\|\widehat{\mathbf{x}}_{(\kappa)}\right\|_2^2,
\end{aligned}$$

which leads to Lemma 2. Finally, we obtain the MSE by

combine the bias term and the variance term,

$$\begin{aligned}
& \mathbb{E}\left\|\mathbf{x}^*-\mathbf{x}\right\|_2^2 \\
= \;& \left\|\mathbb{E}\mathbf{x}^*-\mathbf{x}\right\|_2^2+\mathbb{E}\left\|\mathbf{x}^*-\mathbb{E}\mathbf{x}^*\right\|_2^2 \\
= \;& \left\|\mathrm{V}_{(-\kappa)}\,\widehat{x}_{(-\kappa)}\right\|_2^2+\mathrm{Tr}\left(\mathrm{U}_{(\kappa)}\,\mathrm{W}_C\,\mathrm{V}_{(\kappa)}\right)-\frac{1}{m}\left\|\widehat{\mathbf{x}}_{(\kappa)}\right\|_2^2 \\
\leq \;& \frac{1}{1+\kappa^{2\beta}}\sum_{k\geq\kappa}\widehat{x}_k^2(1+k^{2\beta})+\mathrm{Tr}\left(\mathrm{U}_{(\kappa)}\,\mathrm{W}_C\,\mathrm{V}_{(\kappa)}\right) \\
\leq \;& \frac{\mu}{1+\kappa^{2\beta}}\left\|\mathbf{x}\right\|_2^2+\mathrm{Tr}\left(\mathrm{U}_{(\kappa)}\,\mathrm{W}_C\,\mathrm{V}_{(\kappa)}\right).
\end{aligned}$$

■

C. Proof of Corollaries 3 and 4

For a type-1 graph, we assume that each element in an approximately bandlimited signal has a similar magnitude. Since all the elements in V have the same magnitude, each element of a graph signal, $x_i=\mathbf{v}_i^T\widehat{\mathbf{x}}$, should have a similar magnitude. In other words, $N\max_i x_i^2$ and $\left\|\mathbf{x}\right\|_2^2$ are of the same order.

For uniform sampling, based on Corollary 1, we have

$$\begin{aligned}
& \frac{\mu}{1+\kappa^{2\beta}}\left\|\mathbf{x}\right\|_2^2+\frac{N}{m}\sum_{k=1}^{\kappa}\sum_{i=1}^{N}\mathrm{U}_{k,i}^2\left(x_i^2+\sigma^2\right) \\
\leq \;& \left\|\mathbf{x}\right\|_2^2\left(\frac{\mu}{\kappa^{2\beta}}+\frac{N\left(\max_i x_i^2+\sigma^2\right)}{m\left\|\mathbf{x}\right\|_2^2}\sum_{k=1}^{\kappa}\sum_{i=1}^{N}\mathrm{U}_{k,i}^2\right) \\
\overset{(a)}{=} \;& \left\|\mathbf{x}\right\|_2^2\left(\frac{\mu}{\kappa^{2\beta}}+\frac{N(\max_i x_i^2+\sigma^2)}{\left\|\mathbf{x}\right\|_2^2}\frac{\kappa}{m}\right) \\
\leq \;& \left\|\mathbf{x}\right\|_2^2\left(\frac{\mu}{\kappa^{2\beta}}+\frac{c\kappa}{m}\right) \\
\asymp \;& C\left\|\mathbf{x}\right\|_2^2 m^{-\frac{2\beta}{2\beta+1}},
\end{aligned}$$

where (a) follows from U being orthornormal, κ being in the order of $m^{\frac{1}{2\beta+1}}$, and $C>0$ some constant. Since at least the sampled projection estimator satisfies this rate of convergence, we have

$$\inf_{(\mathbf{x}^*,\mathcal{M})\in\Theta_{\mathrm{rand}}}\sup_{\mathbf{x}\in\mathrm{ABL}_{\mathrm{A}}(K,\beta,\mu)}\mathbb{E}_{\mathbf{x},\mathcal{M}}\left(\frac{\left\|\mathbf{x}^*-\mathbf{x}\right\|_2^2}{\left\|\mathbf{x}\right\|_2^2}\right)\leq Cm^{-\frac{2\beta}{2\beta+1}}.$$

We next show the lower bound. Based on Theorem 3, we have

$$\begin{aligned}
& \inf_{(\mathbf{x}^*,\mathcal{M})\in\Theta_{\mathrm{rand}}}\sup_{\mathbf{x}\in\mathrm{ABL}_{\mathrm{A}}(K,\beta,\mu)}\mathbb{E}_{\mathbf{x},\mathcal{M}}\left(\left\|\mathbf{x}^*-\mathbf{x}\right\|_2^2\right) \\
\geq \;& \frac{c_1\mu\left\|\mathbf{x}\right\|_2^2}{\kappa_0^{2\beta}}\left(1-\frac{c\mu\left\|\mathbf{x}\right\|_2^2}{\sigma^2\kappa_0^{2\beta+2}}\left\|\mathrm{V}_{(2,\kappa_0)}\right\|_F^2 m\right), \\
= \;& \frac{c_1\mu\left\|\mathbf{x}\right\|_2^2}{\kappa_0^{2\beta}}\left(1-\frac{c\mu\left\|\mathbf{x}\right\|_2^2}{\sigma^2\kappa_0^{2\beta+1}N}m\right) \\
\geq \;& \frac{c_1\mu\left\|\mathbf{x}\right\|_2^2}{\kappa_0^{2\beta}}\left(1-\frac{c\mu\max_i x_i^2}{\sigma^2\kappa_0^{2\beta+1}}m\right) \\
\asymp \;& c\left\|\mathbf{x}\right\|_2^2 m^{-\frac{2\beta}{2\beta+1}},
\end{aligned}$$

where κ_0 is in the order of $m^{\frac{1}{2\beta+1}}$.

For optimal sampling scores based sampling, based on Corollary 2, we have

$$\begin{aligned}
& \frac{\mu}{1+\kappa^{2\beta}}\left\|\mathbf{x}\right\|_2^2+\frac{1}{m}\left(\sum_{i=1}^{N}\sqrt{\sum_{k=1}^{\kappa}\mathrm{U}_{k,i}^2\left(x_i^2+\sigma^2\right)}\right)^2 \\
\leq \;& \left\|\mathbf{x}\right\|_2^2\left(\frac{\mu}{1+\kappa^{2\beta}}+\frac{1}{m}\frac{\max_i x_i^2+\sigma^2}{\left\|\mathbf{x}\right\|_2^2}\left\|\mathrm{U}_{(\kappa)}\right\|_{2,1}\right) \\
\overset{(a)}{\leq} \;& \left\|\mathbf{x}\right\|_2^2\left(\frac{\mu}{1+\kappa^{2\beta}}+\frac{\max_i x_i^2+\sigma^2}{\left\|\mathbf{x}\right\|_2^2}\frac{N\kappa}{m}\right) \\
\asymp \;& C\left\|\mathbf{x}\right\|_2^2 m^{-\frac{2\beta}{2\beta+1}},
\end{aligned}$$

where (a) follows from that, based on Definition 5, $\left\|\mathrm{U}_{(\kappa)}\right\|_{2,1}^2=\left(N\sqrt{\kappa(\frac{c}{\sqrt{N}})^2}\right)^2=O(N\kappa)$, which is of the same order of $N\left\|\mathrm{U}_{(\kappa)}\right\|_F^2$. Since at least the sampled projection estimator satisfies this rate of convergence, we have

$$\inf_{(\mathbf{x}^*,\mathcal{M})\in\Theta_{\exp}}\sup_{\mathbf{x}\in\mathrm{ABL}_{\mathrm{A}}(K,\beta,\mu)}\mathbb{E}_{\mathbf{x},\mathcal{M}}\left(\frac{\left\|\mathbf{x}^*-\mathbf{x}\right\|_2^2}{\left\|\mathbf{x}\right\|_2^2}\right)\leq Cm^{-\frac{2\beta}{2\beta+1}}.$$

Based on Definition 5, $\left\|\mathrm{V}_{(2,\kappa_0)}\right\|_{\infty,2}^2=\kappa_0(\frac{c}{\sqrt{N}})^2=c^2\kappa_0/N$, which is of the same order of $\left\|\mathrm{V}_{(2,\kappa_0)}\right\|_F^2/N$, we have

$$\begin{aligned}
& \inf_{(\mathbf{x}^*,\mathcal{M})\in\Theta_{\exp}}\sup_{\mathbf{x}\in\mathrm{ABL}_{\mathrm{A}}(K,\beta,\mu)}\mathbb{E}_{\mathbf{x},\mathcal{M}}\left(\left\|\mathbf{x}^*-\mathbf{x}\right\|_2^2\right) \\
\geq \;& \frac{c_1\mu\left\|\mathbf{x}\right\|_2^2}{\kappa_0^{2\beta}}\left(1-\frac{c\mu\left\|\mathbf{x}\right\|_2^2}{\sigma^2\kappa_0^{2\beta+2}}\left\|\mathrm{V}_{(2,\kappa_0)}\right\|_{\infty,2}^2 m\right), \\
= \;& \frac{c_1\mu\left\|\mathbf{x}\right\|_2^2}{\kappa_0^{2\beta}}\left(1-\frac{c\mu\left\|\mathbf{x}\right\|_2^2}{\sigma^2\kappa_0^{2\beta+1}N}m\right) \\
\geq \;& \frac{c_1\mu\left\|\mathbf{x}\right\|_2^2}{\kappa_0^{2\beta}}\left(1-\frac{c\mu\max_i x_i^2}{\sigma^2\kappa_0^{2\beta+1}}m\right) \\
\asymp \;& c\left\|\mathbf{x}\right\|_2^2 m^{-\frac{2\beta}{2\beta+1}},
\end{aligned}$$

where κ_0 is in the order of $m^{\frac{1}{2\beta+1}}$. ■

D. Proof of Corollaries 5 and 6

For a type-2 graph, we assume that a few elements in an approximately bandlimited signal have much higher magnitudes than the others. The intuition is that, since V is sparse, the energy concentrates in $O(\kappa)$ rows of $\mathrm{V}_{(\kappa)}$, thus, $O(\kappa)$ components of an approximately bandlimited signal, $x_i\approx\mathbf{v}_{i,(\kappa)}^T\widehat{\mathbf{x}}_{(\kappa)}$, have much higher magnitudes than the others. In other words, $\kappa\max_i x_i^2$ and $\left\|\mathbf{x}\right\|_2^2$ are of the same order.

For uniform sampling, based on Corollary 1, we have

$$\begin{aligned}
&\frac{\mu}{1+\kappa^{2\beta}}\left\|\mathbf{x}\right\|_2^2+\frac{N}{m}\sum_{k=1}^{\kappa}\sum_{i=1}^{N}\mathrm{U}_{k,i}^2\left(x_i^2+\sigma^2\right)\\
\leq\;&\left\|\mathbf{x}\right\|_2^2\left(\frac{\mu}{\kappa^{2\beta}}+\frac{N\left(\max_i x_i^2+\sigma^2\right)}{m\left\|\mathbf{x}\right\|_2^2}\sum_{k=1}^{\kappa}\sum_{i=1}^{N}\mathrm{U}_{k,i}^2\right)\\
=\;&\left\|\mathbf{x}\right\|_2^2\left(\frac{\mu}{\kappa^{2\beta}}+\frac{N(\max_i x_i^2+\sigma^2)}{\kappa\max_i x_i^2}\frac{\kappa}{m}\right)\\
\leq\;&\left\|\mathbf{x}\right\|_2^2\left(\frac{\mu}{\kappa^{2\beta}}+\frac{cN}{m}\right)\\
\asymp\;&C\left\|\mathbf{x}\right\|_2^2 m^{-\frac{2\beta}{2\beta+\gamma}},
\end{aligned}$$

where γ varies with κ to satisfy $\kappa^\gamma\leq N$ ($\gamma>1$) and κ is in the order of $m^{\frac{1}{2\beta+\gamma}}$, and $C>0$ is some constant. Since at least Algorithm 1 satisfies this rate of convergence, we thus have

$$\inf_{(\mathbf{x}^*,\mathcal{M})\in\Theta_{\mathrm{rand}}}\sup_{\mathbf{x}\in\mathrm{ABL}_{\mathrm{A}}(K,\beta,\mu)}\mathbb{E}_{\mathbf{x},\mathcal{M}}\left(\left\|\mathbf{x}^*-\mathbf{x}\right\|_2^2\right)\leq Cm^{-\frac{2\beta}{2\beta+\gamma}}.$$

We next show the lower bound. Based on Theorem 3, we have

$$\begin{aligned}
&\inf_{(\mathbf{x}^*,\mathcal{M})\in\Theta_{\mathrm{rand}}}\sup_{\mathbf{x}\in\mathrm{ABL}_{\mathrm{A}}(K,\beta,\mu)}\mathbb{E}_{\mathbf{x},\mathcal{M}}\left(\left\|\mathbf{x}^*-\mathbf{x}\right\|_2^2\right)\\
\geq\;&\frac{c_1\mu\left\|\mathbf{x}\right\|_2^2}{\kappa_0^{2\beta}}\left(1-\frac{c\mu\left\|\mathbf{x}\right\|_2^2}{\sigma^2\kappa_0^{2\beta+2}N}\left\|\mathrm{V}_{(2,\kappa_0)}\right\|_F^2 m\right),\\
=\;&\frac{c_1\mu\left\|\mathbf{x}\right\|_2^2}{\kappa_0^{2\beta}}\left(1-\frac{c\mu\kappa_0\max_i x_i^2}{\sigma^2\kappa_0^{2\beta+1}N}m\right)\\
=\;&\frac{c_1\mu\left\|\mathbf{x}\right\|_2^2}{\kappa_0^{2\beta}}\left(1-\frac{c\mu\max_i x_i^2}{\sigma^2\kappa_0^{2\beta+\gamma}}m\right)\\
\asymp\;&cm^{-\frac{2\beta}{2\beta+\gamma}},
\end{aligned}$$

where κ_0 is in the order of $m^{\frac{1}{2\beta+\gamma}}$.

For optimal sampling scores based sampling, based on Corollary 2, we have

$$\begin{aligned}
&\frac{\mu}{1+\kappa^{2\beta}}\left\|\mathbf{x}\right\|_2^2+\frac{1}{m}\left(\sum_{i=1}^{N}\sqrt{\sum_{k=1}^{\kappa}\mathrm{U}_{k,i}^2\left(x_i^2+\sigma^2\right)}\right)^2\\
\leq\;&\left\|\mathbf{x}\right\|_2^2\left(\frac{\mu}{1+\kappa^{2\beta}}+\frac{1}{m}\frac{\max_i x_i^2+\sigma^2}{\left\|\mathbf{x}\right\|_2^2}\left\|\mathrm{U}_{(\kappa)}\right\|_{2,1}^2\right)\\
\overset{(a)}{\leq}\;&\left\|\mathbf{x}\right\|_2^2\left(\frac{\mu}{1+\kappa^{2\beta}}+\frac{\max_i x_i^2+\sigma^2}{\left\|\mathbf{x}\right\|_2^2}\frac{\kappa^2}{m}\right)\\
=\;&\left\|\mathbf{x}\right\|_2^2\left(\frac{\mu}{1+\kappa^{2\beta}}+\frac{\max_i x_i^2+\sigma^2}{\kappa\max_i x_i^2}\frac{\kappa^2}{m}\right)\\
\asymp\;&C\left\|\mathbf{x}\right\|_2^2 m^{-\frac{2\beta}{2\beta+1}},
\end{aligned}$$

where (a) follows from the energy concentrating in $O(\kappa)$ columns of $\mathrm{U}_{(\kappa)}$ as shown in Definition 6 and the upper bound reaching the minimum when κ is in the order of $m^{\frac{1}{2\beta+1}}$. Since at least Algorithm 1 satisfies this rate of convergence, we have

$$\inf_{(\mathbf{x}^*,\mathcal{M})\in\Theta_{\exp}}\sup_{\mathbf{x}\in\mathrm{ABL}_{\mathrm{A}}(K,\beta,\mu)}\mathbb{E}_{\mathbf{x},\mathcal{M}}\left(\left\|\mathbf{x}^*-\mathbf{x}\right\|_2^2\right)\leq Cm^{-\frac{2\beta}{2\beta+1}}.$$

Based on Definition 6, $\left\|\mathrm{V}_{(2,\kappa_0)}\right\|_{\infty,2}^2=c$, we have

$$\begin{aligned}
&\inf_{(\mathbf{x}^*,\mathcal{M})\in\Theta_{\exp}}\sup_{\mathbf{x}\in\mathrm{ABL}_{\mathrm{A}}(K,\beta,\mu)}\mathbb{E}_{\mathbf{x},\mathcal{M}}\left(\left\|\mathbf{x}^*-\mathbf{x}\right\|_2^2\right)\\
\geq\;&\frac{c_1\mu\left\|\mathbf{x}\right\|_2^2}{\kappa_0^{2\beta}}\left(1-\frac{c\mu\left\|\mathbf{x}\right\|_2^2}{\sigma^2\kappa_0^{2\beta+2}}\left\|\mathrm{V}_{(2,\kappa_0)}\right\|_{\infty,2}^2 m\right),\\
=\;&\frac{c_1\mu\left\|\mathbf{x}\right\|_2^2}{\kappa_0^{2\beta}}\left(1-\frac{c\mu\kappa_0\max_i x_i^2}{\sigma^2\kappa_0^{2\beta+2}}m\right)\\
\asymp\;&cm^{-\frac{2\beta}{2\beta+1}}.
\end{aligned}$$

■